EXPLORING HYBRID NETWORK FOR SEIZURE DETECTION: AN ADVANCED STUDY OVER ELECTROENCEPHALOGRAM SPECTROGRAM

ZENG ZIYI

XIAMEN UNIVERSITY MALAYSIA

2024

XIAMEN UNIVERSITY MALAYSIA
厦門大學馬來西亞分校

FINAL YEAR PROJECT REPORT

EXPLORING HYBRID NETWORK FOR SEIZURE DETECTION: AN ADVANCED STUDY OVER ELECTROENCEPHALOGRAM SPECTROGRAM

NAME OF STUDENT	:	ZENG ZIYI
STUDENT ID	:	CME1909120
SCHOOL/ FACULTY	:	SCHOOL OF COMPUTING AND DATA SCIENCE
PROGRAMME	:	BACHELOR OF ENGINEERING IN SOFTWARE ENGINEERING (HONOURS)
INTAKE	:	2020/09
SUPERVISOR	:	Dr. GOH SIM KUAN

AUGUST 2024

DECLARATION

I hereby declare that this project report is based on my original work except for citations and quotations which have been duly acknowledged. I also declare that it has not been previously and concurrently submitted for any other degree or award at Xiamen University Malaysia or other institutions.

Signature : 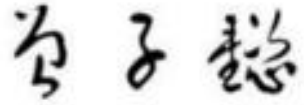

Name : ZENG ZIYI

ID No. : CME1909120

Date : June 5, 2024

APPROVAL FOR SUBMISSION

I certify that this project report entitled "**EXPLORING HYBRID NETWORK FOR SEIZURE DETECTION: AN ADVANCED STUDY OVER ELECTROENCEPHALOGRAM SPECTROGRAM**" that was prepared by ZENG ZIYI has met the required standard for submission in partial fulfillment of the requirements for the award of Bachelor of Engineering in Software Enginnering (Honours) at Xiamen University Malaysia.

Approved by,

Signature : _____

Supervisor : Dr. Goh Sim Kuan

Date : _____

This thesis is a gift for my graduation.

ACKNOWLEDGEMENTS

Fulfilling the completion of this thesis, I realize it’ s time to graduate. Take this opportunity, I wish to express my deepest gratitude to all those who have supported and encouraged me during my bachelor time.

First, I would like to extend my heartfelt thanks to my mentor in Xiamen University Malaysia (XMUM), Dr. Goh Sim Kuan. Since my junior year, he has provided me with unwavering guidance and support along my academic path. As my lecturer for the data mining course, he not only imparted valuable knowledge but also played a crucial role in guiding my graduation thesis. I still remember the time when I proposed the idea of undertaking an academic internship at Westlake University, he provided me with full support and encouragement, this experience that later proved invaluable in my research work.

Furthermore, I want to thank the members of the Cenbrain Laboratory of Westlake University (WU), especially Xurong, Yingjue for the assistance and kindly support during my research time in the internship. I also would like to share my appreciation for my supervisor in WU, Prof.Sawan and Dr. Chen. They generously shared their research experiences and patiently guided me on conducting experiments. With their help, I not only acquired more professional knowledge at that time but also laid the groundwork for writing this thesis even a year later.

Foremost, I would like to express special gratitude to my great family. They have offered unconditional support and understanding for every decision I've made. From leaving home for higher education to studying abroad thousands of miles away, and later transitioning into the field of computer and AI, they have always been my solid support team. Their support has empowered me to pursue my dreams, and I will forever be grateful for this.

Finally, I wish to express my heartfelt appreciation to my friends. I would like to thank their unwavering support and companionship that I have achieved outstanding grades and filled my university experience with joy and warmth. However, some of my friends have already graduated before me, I miss them so much.

Forever embraced with Fortune and Happiness as we can. (愿你我皆被幸福包围！）

ABSTRACT

Automatic seizure detection algorithms have become a research hotspot these years. As a key metric, detection latency is often neglected, which directly affects the timeliness of medical intervention. This work developed three types of Feature Extractors (FE), namely convolution (Conv), recurrent (Rec) and transformer (Transf) for extracting EEG information, with two different time scales. Experiments show that increasing the scale of the Conv and Rec FEs only marginally improves the detection latency, with no such benefit seen for the Transf FE. Subsequently, our work further introduced hybrid FE based on 2 individual FE. The result shows the both the feature fusion and the shorter slicing windows will significantly improve detection latency. The present method achieves 1.82 seconds in epilepsy detection latency, which is the current SOTA score.

Moreover, a closed-loop neuroimaging monitoring system (C-RNMS) is implemented to solve the urgent need of epilepsy patients. Based on Arduino hardware, this system can receive and process electrical signals in real time via a mobile application, which meets the multiple needs of people with epilepsy and lowers the threshold for them and their caregivers to access and monitor brain signals. The findings of this research are expected to provide new insights and ideas for epilepsy detection.

Keyword: Epilepsy Detection, Hybrid Feature Extractor Design, Internet of Thing, Mobile Application Design

Table of Contents

LIST OF TABLES

LIST OF FIGURES

LIST OF SYMBOLS / ABBREVIATIONS

Acc	Accuracy
Sen	Sensitivity
F1	F1 Score
AUROC	Area Under ROC Curve
AP	Average Precision
STFT	Short Time Fourier Transform
FE	Feature Extractor
Conv	Convolution Feature Extractor
Rec	Recurrent Feature Extractor
Transf	Transformer Feature Extractor
EEG	Electroencephalogram
FMRI	Functional Magnetic Resonance Imaging
DL	Deep Learning
RNMS	Real-Time Neuroimaging Monitoring System
Q-Q	Quantile-Quantile
BCE loss	Binary Cross Entropy Loss
ILAE	International League Against Epilepsy
ReLU	Rectified Linear Unit
AI	Artificial Intellegence
Lat	Detection Latency

Chapter 1: Introduction

This chapter, which serves as the opening of the thesis, will provide a brief introduction to the following three topics: symptoms and mechanisms of epilepsy, the cutting-edge neuroimaging techniques with epilepsy diagnosis, and the status of seizure detection algorithms. This chapter aims to provide the reader with an initial understanding of epilepsy disorders and related detection techniques. At the end of this chapter, the contribution and structure of this paper will be elaborated.

1.1 Brain and Epilepsy

"Brain is mysterious." The brain probably is the most complex organ in the human body. It is the center of the nervous system, responsible for regulating basic functions such as movement, cognition and perception (Teng & Kravitz, 2019). As one of the most complex organs in the human body, its intricate structure and function have been a mysterious area of scientific exploration. Brain dysfunction can lead to a wide range of diseases that can seriously affect patients' quality of life and physical health (A. H. Shoeb & Guttag, 2010).

Epilepsy, as a typical neurological disorder, is characterized by recurrent seizures over a short period of time (Xu et al., 2022b). Epilepsy has a significant physical and psychological impact on the patient. Sudden convulsive seizures pose a great risk to the patient, as well as a burden of care for those around them. The type, severity and condition vary greatly among the patients, which makes the accurate diagnosis and treatment much more challenging, especially in the place where medical resources are scarce (T. Liu et al., 2020).

1.2 Neuroimaging Technology

In modern times, the field of neuroscience has developed rapidly. Among them, neuroimaging techniques, as a new diagnostic tool, have been widely used. Among them, Electroencephalogram (*EEG*) and Functional Magnetic Resonance Imaging (*FMRI*), as typical imaging techniques, have made significant contributions to the diagnosis of epilepsy (Balabanov, 2008). *EEG* has been used widely to measure the level of electrical potential on the scalp, while *FMRI* is used to measure changes in blood oxygen levels during brain activity. There have been numerous reports in the literature that when a convulsive seizure occurs in an epileptic patient, the normal way of neuronal activity within the brain is altered, and both the EEG and FMRI can be significantly different from usual at this time. For example, on spectrograms, seizures are most easily recognized by a "flame" pattern of appearance, which is due to a sudden increase in power in a frequency range that is prominent in the background (Sharma et al., 2022).

With the rapid development of technology, Deep Learning (*DL*) has gained popularity and spread in modern society. DL has been widely used in various industries (e.g., natural language processing and computer vision). In the field of neuroscience, DL, through its integration with neuroimaging systems, has shown great potential not only in helping medical professionals in decision making, but also in providing new tools for studying the neural mechanisms of diseases. The time-consuming nature of clinical EEG diagnosis and its variability can be greatly improved by automated seizure classification systems to help professionals (T. Liu et al., 2020).

1.3 Automated Seizure Detection

During a seizure, an individual may lose consciousness and reaching them for help

can be a challenge. This increases the difficulty of treating epilepsy in a timely manner. Therefore, it is necessary for caregivers to monitor individuals with epilepsy to ensure they receive emergency care when needed. In recent years, the use of automated seizure alert systems has received increased attention from researchers as the cost of monitoring has gradually increased. These technologies are expected to perform well in identifying and forecasting epileptic seizures, allowing medical practitioners to intervene sooner and guarantee patient safety. Therefore, as an important component of the system, DL has become a hot research topic in this field in recent years, for how to rationally design the model architecture to improve the diagnostic success rate in epilepsy.

1.4 Problem Statements

In this study focus on the field of epilepsy detection. There are various criteria to evaluate the merit of an algorithm such as false alarm rate (FDR), sensitivity, latency and accuracy. Among these criteria, the detection latency of the algorithm has received a lot of attention from many researchers. Latency time can be defined as the delay incurred by the algorithm to issue an alert after the patient has had a seizure onset. The importance of this metric is that it determines whether we can intervene with the patient in time to avoid possible brain damage or life-threatening situations. However, this important metric is often overlooked in similar studies. Therefore, an in-depth study of it is necessary.

1.5 Aims and Objective

The aim of this study is to shorten the algorithm's detection latency to facilitate the timely medical intervention to epilepsy patients. Specifically, this paper will present and explore various factors that may affect detection latency and evaluate the effect of these factors on detection latency on a publicly available dataset. This study will

make an important contribution to improving epilepsy detection algorithms. To achieve this aim, the study will pursue the following objectives:

- To investigate the impact of different structure and scale in reducing detection latency
- To explore the potential of hybrid feature extractor (FE) architectures in reducing detection latency
- To evaluate the effectiveness on the length of EEG slicing windows in reducing detection latency
- To develop a close-loop Internet of Thing (IOT) system for real-time neuroimaging monitoring

1.6 Overview of Contribution

The main contributions of this final year project are:

- Proposed three different structure feature extractors (FEs) based on existing works with two scales.
- Demonstration that the scale of FE has a not significant improvement on detection latency.
- Evidence that the stability of large models decreases under few-sample training.
- Proposal of a feature extractor fusion framework and proof that the mixed feature extractors can slightly improve model performance.
- First demonstration that the size of the sliding window can significantly improve epilepsy detection delay, achieving an effect of 49%.
- Proposal of a closed-loop neuroimaging monitoring system, including circuit design and mobile application design.

1.7 Thesis Overview

The content of this thesis is organized as below:

- **Chapter 1** introduces the research background, typical neuroimaging techniques, the application scenarios and status of epilepsy automatic detection algorithms and provides an overview of the thesis structure.
- **Chapter 2** reviews the existing work in the field of epilepsy, covering common types of deep learning tasks, typical feature forms, and typical structures. It also discusses the advantages and limitations of various studies.
- **Chapter 3** presents improvements to three existing feature extractor structures and proposes a general framework for feature fusion. Other experimental design details are also included in this chapter.
- **Chapter 4** showcases the research results, with the performance of each feature extractor and the mixed feature extractors tested and displayed.
- **Chapter 5** discusses the experimental results, comparing them with state-of-the-art work. The limitations of this study are also addressed.
- **Chapter 6** proposes a closed-loop neuroimaging monitoring system(C-RNMS) for epilepsy-care, with the name “Neuro-Safe”. This system aims to bringing the gospel to epilepsy patients, which includes three sub-modules: local hardware design, cloud computing, and a mobile application.
- **Chapter 7** provides a comprehensive summary of this research work and offers prospects for future developments.

Chapter 2: Literature Review

Chapter 2 provides a comprehensive review of existing research in the field of epilepsy, covering common deep learning task types, typical feature forms, and common network structures. This chapter also discusses the strengths and weaknesses of various studies and provides a reference point for subsequent improvements by comparatively analyzing the performance and applicability scenarios of different methods. Meanwhile, this chapter points out that epilepsy detection latency is an important but often overlooked metric. Finally, the chapter suggests several factors that may affect detection delay and provides corresponding solutions. The content of this section helps readers to have a comprehensive understanding of the current state of research and the direction of technology development in the field of automatic epilepsy detection.

2.1 Electroencephalogram

Electroencephalogram (*EEG*) is a combination of a voltmeter and an amplifier (Beniczky & Schomer, 2020a), and the electrical signals recorded by EEG are generated by those neurons in the cerebral cortex which firing with each other (Schomer & Silva, 2012). EEG is an important and relatively inexpensive tool compared to FMRI, while it allows intensive care physicians to monitor the brain activity of critically ill patients in real time (Sharma et al., 2022). There are two types of EEG according to the location of EEG acquisition, called Intracranial and Scalp. Among them, the signal acquisition on the Scalp is the most common type of electrode. The electrodes are usually composed of inert silver chloride to maximize the avoidance of electromagnetic interference (Sharma et al., 2022). Acquisition with electrodes embedded subcutaneously is also available, however the acceptance rate is relatively low as it requires invasive surgery.

The electrode arrangement for EEG generally adheres to the International 10-20 System. Specifically, the electrodes are named by the head region abbreviation and number. Abbreviations used on EEG include Fp (frontal pole), F (frontal lobe), C (central lobe), P (parietal lobe), O (occipital lobe), T (temporal lobe), and so on (Beniczky & Schomer, 2020b).

2.2 Difficulties in Diagnosing Epilepsy

It has been demonstrated that EEG is useful in the diagnosis of a variety of disorders, including epilepsy (T. Liu et al., 2020; Xu et al., 2020, 2024), addiction (Chen et al., 2023; D.-X. Li et al., 2023), PTSD (Pelin et al., 2021), and a wide range of other psychiatric disorders (T. Wang et al., 2023). This is because neuronal damage caused by brain disorders can gradually be reflected on the EEG and distinguish with healthy human. The efficiency of EEG emphasizes its critical importance in the clinical evaluation and treatment of brain disorders. It not only provides valuable insights into the pathogenesis of these disorders, but also aids in accurate diagnosis and prognosis.

In the past, direct clinical observation was the gold standard for diagnosing seizures. However, some clinical manifestations of epilepsy can be subtle (Massey et al., 2018), and some patients do not even realize they have epilepsy (Noachtar, 2018). Video-EEG has been shown to be indispensable in confirming the diagnosis of epilepsy when the clinical basis for the diagnosis is not reliable (T. Liu et al., 2020). In fact, many seizures (most prominent in newborns) are only visible on the EEG (Massey et al., 2018). As a result, many clinicians are increasingly focusing on EEG data to identify seizures in their patients. EEG has gradually replaced clinical observation as the new diagnostic standard (Shellhaas, 2015).

However, the use of EEG for epilepsy diagnosis also faces difficulties. First, EEG can be affected by electromagnetic interference in the surrounding area.

Electromagnetic interference can form artifacts on the EEG, causing contamination. Although several methods have been invented in recent years to remove external influences from the EEG, such as independent component analysis (Hyvärinen & Oja, 2000), it is still not completely eradicated. Secondly, even experienced physicians may miss subtle changes in the raw EEG trends and lead to misdiagnosis (Panayiotopoulos, 2005a). A definitive diagnosis of epilepsy requires definitive EEG segments, yet people with epilepsy have convulsions that come on at irregular intervals, and finding and interpreting EEG segments after the fact is labor-intensive. All of this points to the immediate need for epilepsy prediction beforehand and timely detection during seizures (Burton, 2018).

Correct diagnosis of seizure type is crucial as it directly affects the choice of therapeutic medication and the provision of prognostic information (Goldenberg, 2010). The International League Against Epilepsy (*ILAE*) categorizes epilepsy types into the following categories based on differences (Fisher et al., 2017):

2.3 Type of Epilepsy with EEG Feature

- Focal Epilepsy: abnormal discharges are confined to specific areas of the brain, patient may remain awake during the seizure.
- Generalized Epilepsy: discharge usually involves both sides of the brain and is the more common type of epilepsy.
- Unknown Epilepsy: unclear on the discharges region and requires further diagnosis and evaluation.

However, these classes of epilepsy are very similar in clinical symptoms and are difficult to distinguish precisely for symptomatic treatment (Panayiotopoulos, 2005b). The use of EEG helps to distinguish them precisely at this point (T. Liu et al., 2020). For example, patients with focal epilepsy have seizures in which only some of the

EEG channels show significant fluctuations. This contrasts with the situation in patients with generalized epilepsy, where all EEG channels fluctuate abnormally during an attack. In this case, doctors can use the EEG to more accurately classify and diagnose the type of epilepsy and provide more precise treatment for the patient.

2.4 Advanced Deep Learning Technology

2.4.1 Seizure Duration and Machine Learning Task

The different stages (period) in EEG are in are usually categorized as follows:

- Ictal: the period when patient is experiencing seizures onset. The EEG usually shows abnormal electrical activity (such as high amplitude). The duration when the EEG becomes abnormal and clinical symptoms often correspond perfectly to each other.
- Interictal: the period between two seizures. In this period, the patient usually shows no clinical symptoms. No abnormal in EEG as well.
- Postictal: the period after a seizure. the EEG still shows a small amount of abnormal EEG signals.
- Preictal: the period before a seizure. The patient does not experience symptoms and the EEG may show abnormal electrical signals.

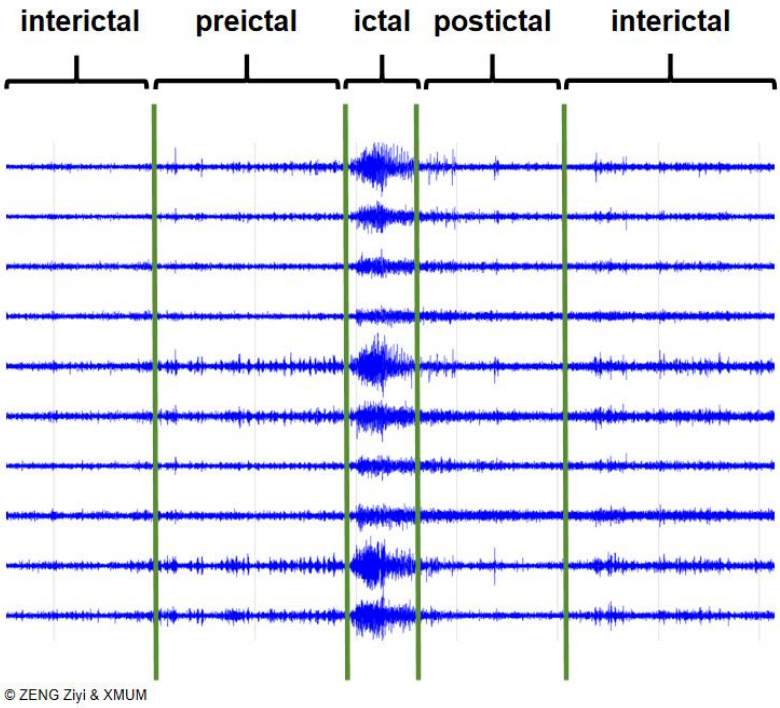

Figure 2.1: Time division of one seizure

Concerning the temporal division of the various stages of epilepsy, the Ictal stage is relatively accurate, because it can be divided according to the time point of the symptoms. However, time division for the other stages is relatively subjective. For example, many works default the Preictal time to 30 minutes before the onset of epilepsy (Hu et al., 2023; Truong et al., 2018; Xu et al., 2020), while others set it to 60 minutes (Myers et al., 2016).

Currently, algorithmic research in epilepsy can be categorized into a total of three task types, namely: seizure detection, prediction and classification. The following table shows in detail the goals and classic papers for each type of task. In the past, researchers have tended to study algorithms for Seizure detection, where the goal is for the algorithm to identify, as much as possible, the epilepsy that is occurring. As shown in Figure 2.1, the idea of seizure detection is to distinguish the preictal clip from the ictal clip.

However, the task of seizure prediction and classification piqued the interest of researchers. The goal of Seizure prediction is to predict impending epilepsy to alert medical personnel to intervene in a timely manner. Unlike with detection, the ideas of prediction is to distinguish the interictal clip with preictal. Usually, when

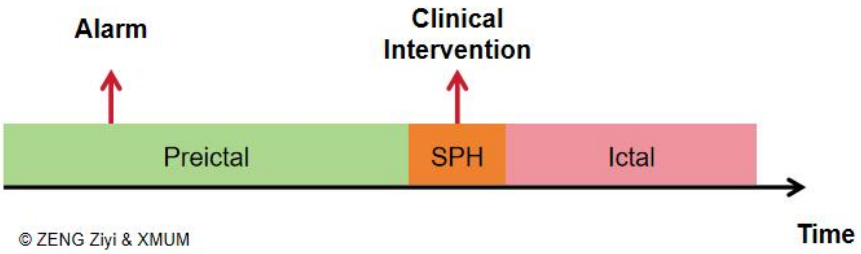

Figure 2.2: Definition of preictal, SPH, and ictal

determining the training samples, researchers also need to consider a realistic factor that patients and doctors should be given a reaction time before a seizure occurs, called seizure prediction horizon (SPH) (Hu et al., 2023). SPH ensures that medical personnel can have time to react and commit to treatment. The SPH time definition is also quite subjective, but most work defines it as 5 minutes (Hu et al., 2023; Xu et al., 2020).

As for seizure classification, it aims to classify the type of seizure given one EEG clip. However, in context of seizure classification task, it relies on fully labelled EEG data, and relevant datasets have been missing in the past, this has led to difficulties in conducting relevant research. Although relevant datasets, for example, TUSZ (Shah et al., 2018) have been released in recent years, epilepsy classification has not yet become mainstream as of today. Details related to datasets will be discussed in depth in subsequent sections.

Direction	Goal	Typical Paper
Seizure detection	Detect whether the seizure onset	(Birjandtalab et al., 2017; Hassan et al., 2020; Z. Li et al., 2022; A. Shoeb et al., 2004; A. H. Shoeb & Guttag, 2010; L. S. Vidyaratne & Iftekharuddin, 2017; Xu et al., 2024)
Seizure prediction	Predict the seizure onset in future	(Xu et al., 2020, 2022a; Yan et al., 2022; Zhao et al., 2020, 2022)
Seizure classification	Predict seizure type	(Fisher et al., 2017; M. Liu et al., 2021; T. Liu et al., 2020; Tang et al., 2021)

Table 2.1: Typical study with related to each direction

2.4.2 Feature Extraction

A detailed EEG feature is crucial for optimising the training effect of the model. EEG signals carry abundant and complex information, so how to effectively extract epilepsy-related features has been a central concern for researchers. In early studies, traditional EEG features (e.g., std, mean, etc.) were widely used to train models. The extraction of traditional EEG features has been further supported with the release of many open-source tools by researchers, such as (Gramfort et al., 2013). Most of these studies have used individual patient-specific feature engineering techniques and have achieved significant results in epilepsy prediction tasks. For example, Zhang's work achieved 100% sensitivity and a very low false alarm rate: 0.05/h by manually selecting features (Zhang & Parhi, 2016). However, this feature engineering technique requires significant costs to select the optimal feature combinations and therefore cannot be generalized across patients. Also, these optimal feature

combinations may lose their superiority over time because of the dynamic changes in the brain (Truong et al., 2018).

With the advancement of deep learning techniques, researchers are becoming aware of the potential of deep neural networks in the field of epilepsy diagnosis. Therefore, they began to turn their attention to novel features that are more suitable for deep learning models, including time-domain features, frequency-domain features, and time-frequency-domain features.

Figure 2.3 demonstrates the visualization of three features forms. Time-domain features usually refer to raw or processed EEG signals, which represent the level of potential at a specific point in time. The time-domain signals are Fourier transformed to obtain frequency-domain signals (Brigham & Morrow, 1967), which reflect the energy distribution of EEG segments at different frequencies. In addition, a signal representation in the time-frequency domain can be obtained by performing a short-time Fourier transform on the time-domain signal (Kehtarnavaz, 2008). Wavelet transform is also one of the commonly used signal processing methods (Debnath & Antoine, 2003).

In terms of conventional features, the work of Shoeb et al. is one of the most representative. They input EEG signals into different filters to obtain the processed signals and then used the energies of the different sub bands as feature input models. This algorithm successfully detected 131 (94%) seizures with a detection latency of 8 seconds (A. Shoeb et al., 2004). Subsequently, further work based on this has been carried out by several studies that have used more comprehensive EEG features and achieved better results.

With the widespread use of convolutional layer-based architectures, many researchers have favored the use of novel features for model training. For example, Xu et al. designed an end-to-end architecture that directly inputs the temporal signals of EEG into the model for training and achieved 98.8% sensitivity in an epilepsy prediction task (Xu et al., 2020). In contrast, Truong et al. performed a short-time Fourier transform of the raw signals to obtain a time-frequency domain

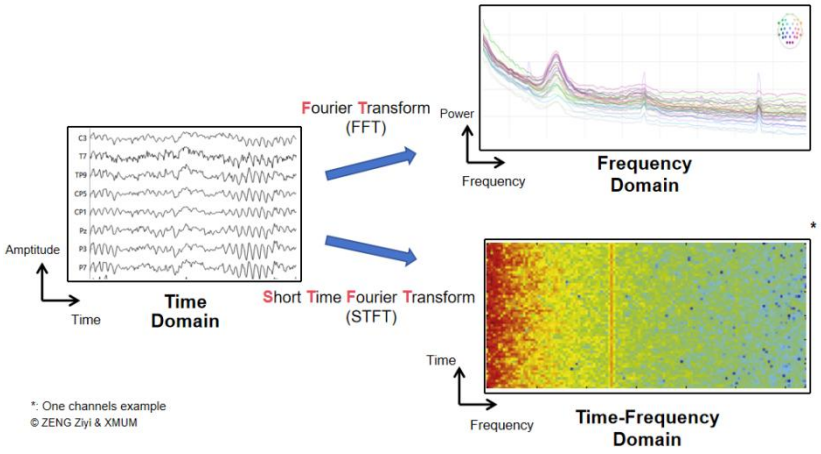

Figure 2.3: Three domain of EEG

representation, and in doing so achieved 78.8% (Truong et al., 2018).

2.4.3 Model architecture

Since the beginning of the last century, a large amount of research on detection algorithms has been introduced. The early classical structures were mainly based on structured data models. These models typically accept structured data and are trained and computed based on multiple features of the data. Typical models include support vector machines and random forests. For example, a 2004 study using support vector machines reported an FDR of 0.25/h (A. Shoeb et al., 2004). Six years later, they released their own dataset, named CHB-MIT, which is now one of the most used datasets (A. H. Shoeb & Guttag, 2010). This research result gave their work a landmark in the field and is considered classic and seminal.

Recently, deep learning (DL) methods have been shown to be able to learn more discriminative feature representations from EEG data. One of the typical model structures is a convolutional layer-based design. This CNN-based architecture is able to process EEG signals as images, using a two-dimensional convolutional kernel to learn relevant features (Xu et al., 2024). As the convolutional layer processes the signal, it slides along both the time and channel dimensions. There have also been many studies using convolutional networks with outstanding results (O'Shea et al., 2020).

However, the drawbacks of the structure of convolutional networks (CNN) come to the fore. Firstly, the use of convolution assumes that the inputs have adjacency. For example, the distance between neighboring pixel points of a picture is the same. In the field of epilepsy research, studies using convolutional layers (Asif et al., 2020; Rasheed et al., 2021; Xu et al., 2020, 2024; Zhao et al., 2020) have defaulted that the EEG signals or spectrograms have a Euclidean architecture. However, this assumption ignores the natural geometry of EEG electrodes and connectivity in brain networks (Tang et al., 2021). In other words, the distances between electrodes are not equal.

The problem faced by convolutional networks can be solved by graph neural networks. Graphs are data structures that can represent complex topologies, and it has been shown that the theory of graphs can be used to model the human brain (Bullmore & Sporns, 2009). At the same time, graphs have been shown to cope with non-topological structures (Chami et al., 2022). Based on this, there are many works that introduce graph machine learning into epilepsy-related research. For example, Tang et al. devised two graph structures and designed a self-training strategy, which eventually achieved 0.767 on seizure classification (Tang et al., 2021).

Furthermore, with the proposal of Transformer (Vaswani et al., 2017), a series of works introduced the self-attention mechanism into this field. For example, Yan et al.

used 3 Transformer blocks as encoders to process the signals and feed them into a decoder for classification. The 3 Transformer encoders in this work processed each of the three dimensions of the spectrograms and ultimately achieved an accuracy of 96.01% (M. Liu et al., 2021).

The composite network structure has naturally attracted the attention of researchers as well, based on the assumption that a single network structure can only extract one-sided features. A working paper found that combining two feature extractors together is beneficial to significantly improve the accuracy of the model (T. Liu et al., 2020). In their experiments, they pre-trained the CNN and RNN networks separately and then combined them together to train them again. Finally, they achieved 97% F1 score on the TUSZ dataset. In addition, Li et al. proposed Graph generative neural network, they combined graph features and convolutional features, and finally obtained a far better score than CNN and GNN (Z. Li et al., 2022).

2.5 Available Dataset

There are many available datasets for seizure detection. Table 2.2 presents detailed information about the current classical open-source datasets, some of whose data are derived from the study of (Wong et al., 2023). It shows a difference in the number of channels in each dataset, which is due to the difference in EEG acquisition systems. An increase in the number of channels implies a higher temporal resolution and spatial coverage capability, which in turn helps to locate the source of the EEG signals more precisely. Moreover, there were inconsistencies in the number of subjects across the datasets, which led to differences in sample sizes. Larger sample sizes can contain richer information and help increase the validity of statistical tests.

The datasets can also be categorised by acquisition location. There are two acquisition locations widely used: scalp and intracranial. Typically, intracranial signals are of better quality than scalp signals because they are closer to the source of

brain activity and are less affected by scalp muscle activity and other external disturbances. From the point of view of data preprocessing, some of the datasets have already undergone preliminary processing. For example, the dataset from the University of Bonn has had artifacts Removed. While other datasets have cut continuous records into shorter segments for subsequent analysis and processing.

Therefore, a high-quality EEG dataset should have the following attributes: multi-channel, multi-sample, and intracranial acquisition methods. To the best of our knowledge, the more popular datasets in the research community include CHB-MIT, TUSZ, and Helsinki. CHB-MIT (A. H. Shoeb, 2009), as a senior dataset, has been widely used in related research fields for decades. And TUSZ (Shah et al., 2018), as an emerging dataset, has gradually gained attention due to its large sample size.

Dataset	Channels Number	Subjects	Location	Remark
University of Bonn	1	10	Scalp/ Intracranial	Artifacts Removed, single channels
CHB-MIT Scalp EEG	18	23	Scalp	Channel unstable
Melbourne-NeuroVista Seizure Trial	16	12	Intracranial	Segmentation
Neurology and Sleep Centre Hauz Khas	1	10	Scalp	Frequency filtered already
TUH EEG Seizure Corpus (TUSZ)	23-31	642	Scalp	Segmentation, large file size
Helsinkl University Hospital EEG	19	79	Scalp	N.A
Siena Scalp EEG	20/29	14	Scalp	N.A

Table 2.2: Open-source dataset of seizure task

2.6 Literature Comparison

When comparing current state-of-the-art technologies in the field of epilepsy prediction and detection, a side-by-side comparison is essential. This careful cross-sectional comparison will help us to better understand the current state-of-the-art in the field of epilepsy prediction and detection and provide useful insights into the direction of future research. The 12 most representative papers (6 prediction, 6 detection) from the literature listed above were included in the evaluation. To assess the strengths and weaknesses of these techniques as comprehensively and objectively as possible, four evaluation metrics were purposely selected: model structure, features, validation, and quality. The sum of all metrics is the final score of the research article. The evaluation criteria and related details are listed below.

- Structures. 1: traditional structures (convolutional and cyclic) used. 2: novel structures used (e.g., self-attention mechanisms). 3: Hybrid structures used
- Features. 1: temporal features used (except for graph structures). 2: frequency domain, time-frequency features, or temporal features (for graph structures) used. 3: hybrid features used
- Validation. 1: not distinguish between training and validation sets. 2: Uses K-fold cross-validation. 3: Leave-one-out or novel methods
- Quality. 1: Published in JCR Q3/Q4 area journals, CCF-C conference, or unclassifiable. 2: Published in JCR Q2 journals, or CCF-B conference. 3: Published in JCR Q1 journals (IF less than 6), CCF-A conference. 4: Published in JCR Q1 area journals (IF greater than or equal to 6)

Structures	Features	Validation	Quality	Total
An End-to-End Deep Learning Approach for Epileptic Seizure Prediction (Xu et al., 2020)				
1	1	2	2	6
Convolutional neural networks for seizure prediction using intracranial and scalp Electroencephalogram (Truong et al., 2018)				
1	2	3	4	10
Multichannel Synthetic Preictal EEG Signals to Enhance the Prediction of Epileptic Seizures (Xu et al., 2022a)				
1	2	3	2	8
Seizure Prediction Based on Transformer Using Scalp Electroencephalogram (Yan et al., 2022)				
2	2	1	2	7
Exploring the Applicability of Transfer Learning and Feature Engineering in Epilepsy Prediction Using Hybrid Transformer Model (Hu et al., 2023)				
3	2	3	3	**11**
Epileptic Seizure Classification with Symmetric and Hybrid Bilinear Models (T. Liu et al., 2020)				
3	2	2	3	10

Table 2.3: Classic work of seizure prediction

Structures	Features	Validation	Quality	Total
Automated EEG-Based Epileptic Seizure Detection Using Deep Neural Networks (Birjandtalab et al., 2017)				
1	2	3	1	7
Graph generative- neural network for EEG - based epileptic seizure detection via discovery of dynamic brain functional connectivity (Z. Li et al., 2022)				
3	2	2	3	**10**
Temporal Graph Convolutional Networks for Automatic Seizure Detection (Covert et al., 2019)				
2	2	3	2	8
Shorter Latency of Real-time Epileptic Seizure Detection via Probabilistic Prediction (Xu et al., 2024)				
1	2	3	3	9
Ensembled Seizure Detection Based on Small Training Samples (Tong et al., 2024)				
1	2	2	3	8
DWT-EMD Feature Level Fusion Based Approach over Multi and Single Channel EEG Signals for Seizure Detection (Jana et al., 2022)				
1	2	1	2	6

Table 2.4: classic work of seizure detection

Regarding the prediction of epilepsy, the classical research conducted by Truong et al. and Hu et al. Truong's group unlocked the way for later studies was the use of a convolutional neural network model to train EEG signal spectrograms. This work proposed to use the Leave One Seizure Out (LOO) validation approach to guarantee the accuracy of the training results (Truong et al., 2018). However, Hu's group developed a hybrid Transformer model that combines CNN and Transformer and is based on the self-attention mechanism. This model effectively extracts characteristics

from various EEG frequency bands. By fine-tuning target subjects and pre-training on a substantial amount of patient data, they confirmed the viability of pre-training in the epilepsy prediction task (Hu et al., 2023). For epilepsy detection, the graph generative neural (GNN) network proposed by Li et al. combines the strengths of CNNs and graph networks, ultimately achieving an impressive F1 score of 0.9.

These investigations demonstrate that composite structures exhibit notable benefits in the realms of epilepsy detection and prediction. This composite structure facilitates the extraction of intricate EEG characteristics for categorization from multidimensional network patterns (T. Liu et al., 2020).

2.7 Hypothesis and Solutions

The detection latency of an algorithm is the result of a combination of factors, and identifying these factors is the first step in this research. The following hypotheses will be investigated in this thesis: does the model structure and scale used by the algorithm affect the detection delay? Does the choice of sliding window length affect the detection delay? Does the decision-making process of the algorithm affect the detection delay?

Inspired by the above studies, an important aim of this study is to explore the potential of model scale and composite architectures for epilepsy detection tasks. Firstly, this work hypothesizes that large-scale Feature Extractor (FE) is more conducive to modelling EEG information, therefore we built two different sizes of FE and conducted a comparative analysis of their performance. By comparing their performances in the seizure detection task, we expect to verify whether large-scale FE can capture complex features in EEG signals more effectively. In addition, this experiment hypothesizes that integrating different types of feature extractors can significantly improve the performance of the model in terms of detection latency, due to the complementary nature of the different structures. To test this hypothesis, we

propose a variety of hybrid FE architectures and conduct detailed experiments on them. These hybrid architectures include a combination of FEs of different sizes and types, aiming to fully utilize the advantages of each to achieve more efficient feature extraction and lower detection latency.

For the sliding window, we first chose a length of 5 seconds, as this is the most common length used today. Most of the experiment will be done with 5 seconds slicing windows. After the best hybrid FE is filtered out, we tried to shorten the window length to 2 seconds, to see if the change of slicing windows will optimize the performance of the model.

In the subsequent sections, we describe the experimental process in detail, including the selection of datasets, construction and training of models, performance evaluation metrics, and analysis of experimental results. Through these attempts, we expect to understand how various factors will affect the key metric of detection delay time and provide useful references for future research.

Chapter 3: Material and Methodology

In this chapter, we provide an in-depth introduction to the experimental methodology to ensure that the reader has a comprehensive understanding of the ideas and approach of this work. This chapter covers several key topics, including the selection and pre-processing of the dataset, the building of the model and its post-processing. Notice that unlike other chapters, the descriptions in this chapter will be detailed and specific rather than general, with purples of fully understanding of reader.

3.1 Material

The algorithm proposed in this experiment will be validated on the CHB-MIT scalp EEG database. The dataset contains data from 24 patients (Chb01-Chb24), where Chb01 and Chb21 are from the same female patient with an 18-month interval. Patient information for Chb24 is not available. Electrode positions in the dataset were arranged according to the international 10-20 system. The dataset contained 17 females and 5 males patients ranging in age from 1.5 to 22 years. Each patient's EEG data was evenly segmented into 1/2/4-hour segments and contained at least one segment of data labelled with epilepsy. EEG signals were sampled at a resolution of 256 Hz, and data from each case may contain a different number of channels. The labelled information for epilepsy is saved as text. The details of the dataset are shown in Table 3.1.

Subject ID	Gender	Age	Record time	Number of Seizure	Subject with Recurrent
Chb01	Female	11.0	40.6	7	No
Chb02	Male	11.0	25.3	3	No
Chb03	Female	14.0	28.0	7	No
Chb04	Male	22.0	155.9	4	No
Chb05	Female	7.0	39.0	5	No

Chb06	Female	1.5	66.7	10	Yes
Chb07	Female	14.5	68.1	3	No
Chb08	Male	3.5	20.0	5	No
Chb09	Female	10.0	67.8	4	No
Chb10	Male	3.0	50.0	7	No
Chb11	Female	12.0	34.8	3	No
Chb12	Female	2.0	23.7	40	Yes
Chb13	Female	3.0	33.0	12	Yes
Chb14	Female	9.0	26.0	8	Yes
Chb15	Male	16.0	40.0	20	Yes
Chb16	Female	7.0	19.0	10	Yes
Chb17	Female	12.0	21.0	3	No
Chb18	Female	18.0	36.0	6	No
Chb19	Female	19.0	30.0	3	No
Chb20	Female	6.0	29.0	8	Yes
Chb21	Female	13.0	33.0	4	No
Chb22	Female	9.0	31.0	3	No
Chb23	Female	6.0	28.0	7	Yes

Table 3.1: Classic Work of Seizure Detection

Consecutive seizures are defined as the occurrence of at least two ictal within a two-hour period. In the epilepsy prediction task, consecutive ictal can lead to wrong selection of preictal segments. This is because the ictal epoch of the previous seizure may be incorrectly considered as the preictal epoch of the subsequent seizure. Therefore, we will not consider and train case data for consecutive seizures. Moreover, this work uses a leave-one-out cross validation (LOOCV) method, where the number of fits in training is equal to the number of their seizures. Thus, approximately 150 model training sessions are required to complete a full algorithm evaluation. We chose the same patients for training as in the classical study (Truong et al., 2018), which are chb01-03, chb05, chb09-10, chb14, and chb18-23.

3.2 Preprocessing

3.2.1 Filtering and Slicing

Firstly, the raw EEG signals are normalized to mitigate the differences between subjects while helping the deep learning model to converge quickly. Z-score normalization is used in this work to obtain a more robust feature representation. Then, filters will be used for cancelling out artifacts in the recorded segments. Other work will use range-based filters to remove noise around 57Hz-63Hz (Bhattacharya et al., 2022; Hu et al., 2023). However, the present work only removes noise at 60Hz because we believe that valid information still exists near the noise point. Subsequently, we sliced the EEG segments using a 5-second window.

3.2.2 Spectrogram Transformation

The Fast Fourier Transform (FFT) is the most efficient technique for converting time series signals into frequency domain signals (Hu et al., 2023). The FFT performed over a continuous window to obtain the Spectrogram is known as Short Time Fourier Transform (STFT) (Kehtarnavaz, 2008). In this study, the STFT was used to perform the transformation and the FFT window size was chosen to be 128.

In the context of slicing windows of 5 seconds (refer to chapter 3.4.1), we can easily obtain the spectrogram $\in \mathbb{R}^{B\times22\times65\times21}$. here, 22 represents the number of EEG channels, 65 represents the frequency domain information vector, and 21 represents the number of windows. The model will learn and fit the spectrogram features in subsequent training to better understand and process the frequency domain information of the EEG signal.

However, as for the selection of 2 seconds slicing windows, will obtain spectrogram $\in \mathbb{R}^{B\times22\times65\times9}$. It is oblivious that the last dimension is shorter because of windows

size(duration), from 21 data-point to 9. The comparison of the spectrogram in different slicing windows can be seen in Figure 3.1.

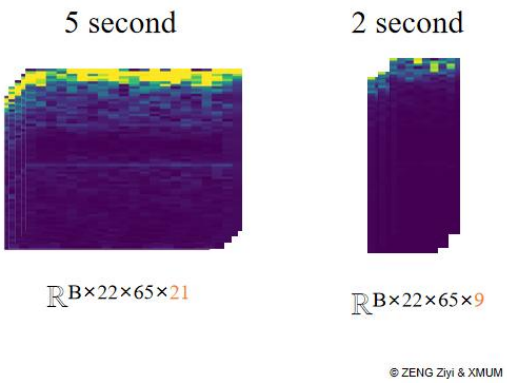

Figure 3.1: Comparison of spectrogram from STFT

3.3 Proposed Feature Extractor

The aim of this study is to develop a generalized structure for epilepsy detection and prediction, which means that the proposed structure should show good performance on both tasks. We propose two model frameworks: a single feature extractor (FE) model structure and a hybrid feature extractor (FE) model structure. Part a) of Fig. 4 illustrates two model structures we proposed. In this structure, the feature map is first passed through the different FE architectures to obtain an implicit representation in the form of R^{Bx768}, where B represents the number of training samples in the batch. This vector is then fed into the classification module to obtain the probability of epilepsy. The FE can be chosen from any of the three classical architectures: Convolution (Conv), Recurrent (Rec) and Transformer (Transf). We have optimised and improved the classical work based on each architecture and tested the improved training results. Also, the size of the FE may affect the training effect, which is included in our study. For the FE of each architecture, we proposed two structures: large and small. These two structures differ by a factor of 5 to 10 in the number of parameters. In the subsequent sections, we will detail each of the proposed models

one by one.

3.3.1 Convolution Feature Extractor

The convolution FE proposed in this work is improved from the model structure from (Truong et al., 2018). In short, we tried to incorporate a residual structure into the original design. By adding jump connections (or called as "shortcut"), the residual structure can successfully solve the problems of gradient vanishing and gradient explosion in deep network learning.

First, the spectrogram goes through an initial block. This block consists of a convolutional layer, a batch normalization layer and a ReLU activation function (refer to following table for more detail). Next, the data will go to the maximum pooling (MP) layer to get the representation as $\mathbb{R}^{B\times768\times3\times3}$. The data then goes to the residual block. Different FE scales use different numbers of residual modules. The smaller scale uses *three* residual modules to get the representation as $\mathbb{R}^{B\times192\times9\times11}$. The larger scale, on the other hand, uses *five* residual modules to obtain a representation of the form $\mathbb{R}^{B\times768\times3\times3}$. Finally, the data goes to the average pooling (AP) and flatten layers to get the output as $\mathbb{R}^{B\times768}$. Details of each layer in the FE are shown in Table 3.2.

Small		**Large**	
Block	Output	Block	Output
Input	(B, 32, 65, 21)	Input	(B, 32, 65, 21)
Initial_Block #1	(B, 32, 65,21)	Initial_Block #1	(B, 32, 65,21)
Max_Polling #1	(B, 32, 32, 21)	Max_Polling #1	(B, 32, 32, 21)
Residual_Block #2	(B, 64, 32, 20)	Residual_Block #2	(B, 64, 32, 21)
Max_Polling #2	(B, 64, 17, 21)	Max_Polling #2	(B, 64, 17, 21)
Residual_Block #3	(B, 128, 17, 21)	Residual_Block #3	(B, 128, 17, 21)
Max_Polling #3	(B, 128, 9, 11)	Max_Polling #3	(B, 128, 9, 11)

Residual_Block #4	(B, 192, 9, 11)	Residual_Block #4	(B, 256, 9,11)
Average_polling	(B, 192, 2, 2)	Max_Polling #4	(B, 256, 5, 6)
Flatten	(B, 768)	Residual_Block #5	(B, 512, 5, 6)
		Max_Polling #5	(B, 512, 3, 3)
		Residual_Block #6	(B, 768, 3, 3)
		Average_polling #6	(B, 768, 1, 1)
		Flatten	(B, 768)
Total Parameters	0.8M	14M	

Table 3.2: Structure of proposed convolution-base network

3.3.4 Recurrent Feature Extractor

The cyclic FE proposed in this study is improved from the model structure adopted by Liu et al. (T. Liu et al., 2020). The original structure used two ConLSTM layers with nine iterations. However, the number of iterations of the loop structure grows linearly with the training time, while the data is difficult to process in parallel, which may become a performance bottleneck.

Figure 3.1a illustrates the proposed recurrent structure in this study, which is characterized by a shorter required time step, thus significantly improving the training speed while considering the performance. Like the original structure, the small-scale FE we designed uses a *one-layer* ConvLSTM. And in order to compare the effect of model size on the training results, for the large-scale FE we designed uses a *two-layer* ConvLSTM. In addition, the dimensions of the hidden layers for the two models are *96* and *192*, respectively. The input data needs to be processed in four-time steps before they are all processed. In the last time step, the FE will output $\in R^{B\times768}$ as a feature representation of the whole FE extraction. The number of parameters for the small scale is 1M, while the number of parameters for the large scale is 6M.

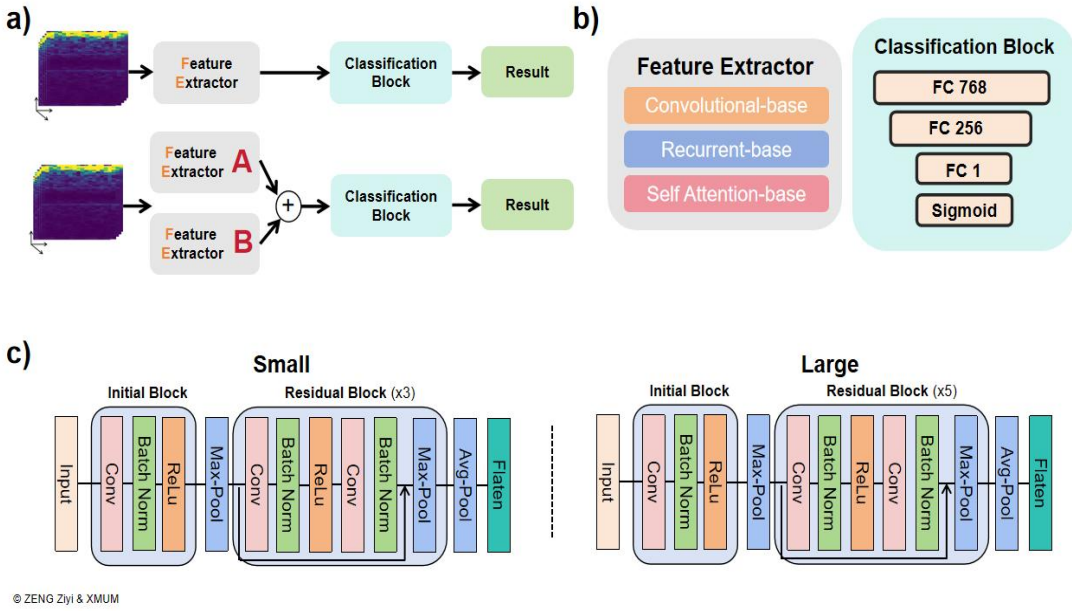

Figure 3.2: Experimental network structure with proposed Convolution FE. a) Single FE and compose FE structure. b) Common block used in network. c) two size of proposed convolution FE

3.3.5 Transformer FE

The recurrent FE proposed in this study is improved from the model structure adopted by Liu et al. (Yan et al., 2022). The original structure uses three Transformer encoder blocks to extract feature information and perform feature fusion in each of the three dimensions of the spectrogram. Each encoder block contains 8 encoders within it, so the whole feature extractor (FE) contains 3*8=24 encoders, which leads to the excessive size of the model.

In our work, we have borrowed the idea of Vision Transformer proposed by (Dosovitskiy et al., 2021) and designed a similar solution. Figure 3.2b illustrates the structure of our proposed model. First, we divide the spectrogram into 21 vectors in the time dimension and then spread it to form 21 tokens, each with a dimension of

1430. Next, we transform the dimensions of the tokens to 768 through a linear projection layer. Then, we splice a randomly generated token with the other tokens to obtain a tensor with the shape (B, 22, 768). This random token is learnable and is often referred to as a "CLS" token, and each token is then passed through a Transformer module, where the output corresponding to the CLS token is taken out and used as the output of the entire FE.

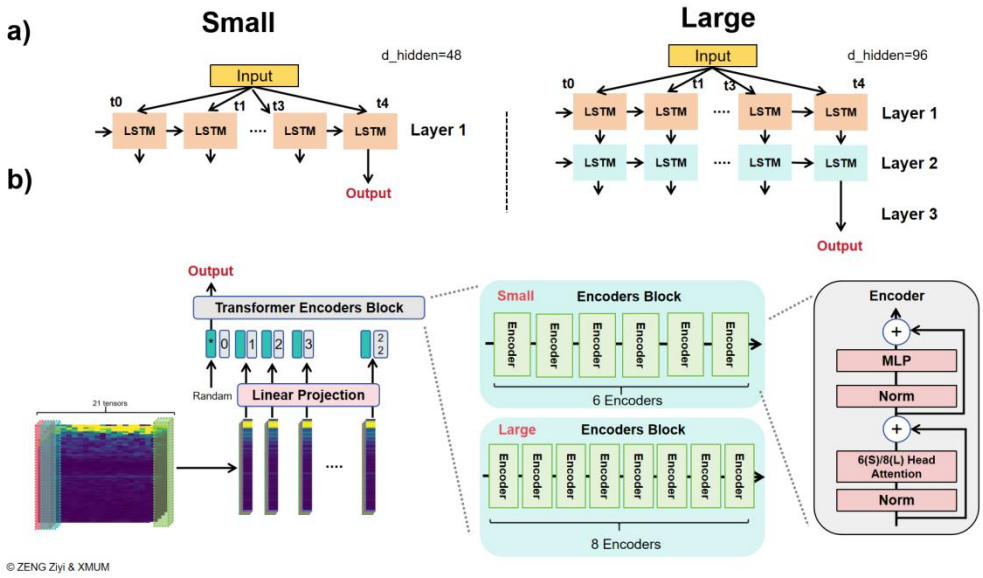

Figure 3.3: Proposed recurrent FE and attention FE. a) Two size of recurrent FE. b) two size of attention FE

Furthermore, the two transformer models we designed are identical in the shape of the input and output tensor. However, the small-scale FE uses *6* encoders for stacking and the large scale uses *8*. Also, the small structure uses a *6-head* self-attention mechanism, and the large structure uses an *8-head* self-attention mechanism. This resulted in a significant difference in their model sizes, with the large model being twice as large as the small model. The number of parameters of the large model is 50M and the number of parameters of the small model is 23M.

3.3.6 Model Size and Training time

Table 3.3 details each model structure and its corresponding statistical information. These statistics include the size of the model and the training time, which usually have a positive relationship with each other. The size of the model directly affects the computational resources required, while the training time reflects the efficiency of the model execution on a particular hardware. In this study, training time is measured in GPU minutes, which represents the total training time for a particular model on an RTX 4060 graphics card. GPU minutes is a commonly used metric that considers the complexity of the model and the performance of the hardware, providing an intuitive metric for evaluating the training cost of a model. The computational methodology is elaborated in Appendix B.

Structure	Size	Trainable Parameter	Estimate Training Time
Convolution FE	Small	0.8M	102.1 min
	Large	14M	153.2 min
Recurrent FE	Small	1M	104.1 min
	Large	7M	123.9 min
Transfermoer FE	Small	23M	195.8 min
	Large	50M	266.6 min

Table 3.3: Model Size and Training time of each FE-base model

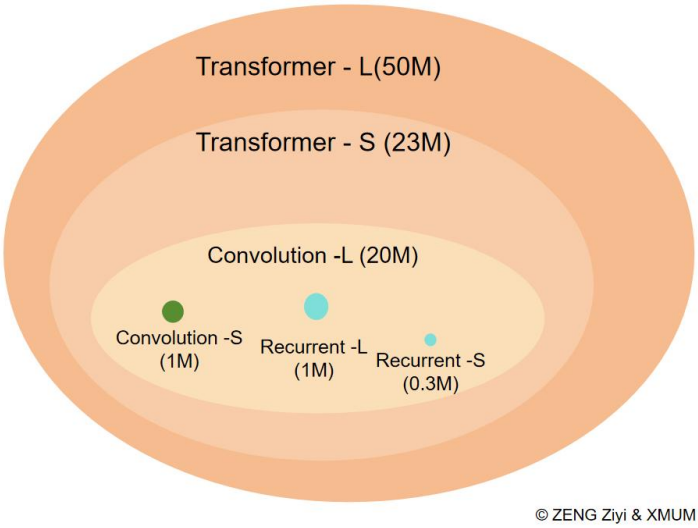

Figure 3.4: Individual FE Model Size Comparison. L:Large, S: Small

3.3.7 Hybrid Feature Extractor Framework Design

Ultimately, we designed a Hybrid Feature Extractor (Hybrid-FE) structure designed to learn different features from the feature map. The fusion model remains identical in all aspects except for the design of the feature extractor (FE). Specifically, the same spectrogram is simultaneously fed into two different FEs, each of which generates a vector with an implicit representation of the form R^{Bx768}. Next, the corresponding positional elements of these two representations are averaged to obtain a vector with the same shape. This fused vector is then fed into the classification module. For a fair comparison, we perform the same training steps.

3.4 Training Setting

3.4.1 Training Set and Slicing Windows

This experiment will focus on the epilepsy detection task and the goal of the model is to differentiate EEG samples from preictal (without SPH) and ictal epochs. This experiment uses leave one seizure out cross validation (LOSOCV). Assuming that

the patient contains n seizures, the model will be trained on n-1 seizure data and then validated on 1 seizure data. Figure 3.4 depicts the division of the training and test

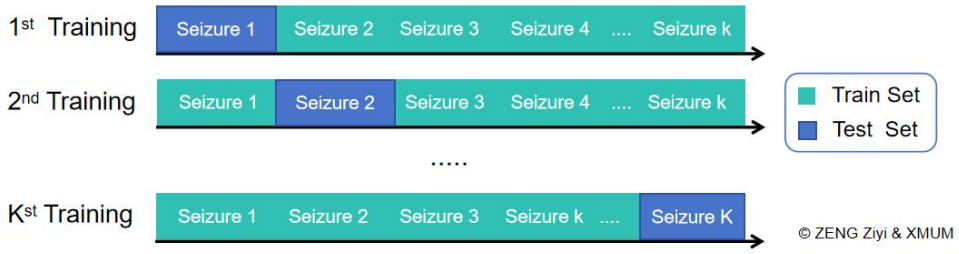

Figure 3.5: Training Set Split

sets in LOSOCV.

In addition, the imbalance of positive and negative samples is a common problem. Since seizures usually occupy a short period of time in the whole EEG signal, it results in a much larger number of negative samples (non-seizure periods) than positive samples (seizure periods). This imbalance causes the model to develop a preference for the majority class during training, which affects the model's performance in real-world scenarios. Truong et al. proposed a method called "Slicing windows". This is a technique to increase the number of negative samples by overlapping sampling techniques during the training phase (Truong et al., 2018).

In this study, we move this window along the time axis of the EEG signal to obtain more samples. To further balance the dataset, we set different slicing steps to the positive sample and negative sample. Figure 3.5 illustrates this 'sliced window' approach, where it can be seen how the window moves along the EEG signal to generate more samples.

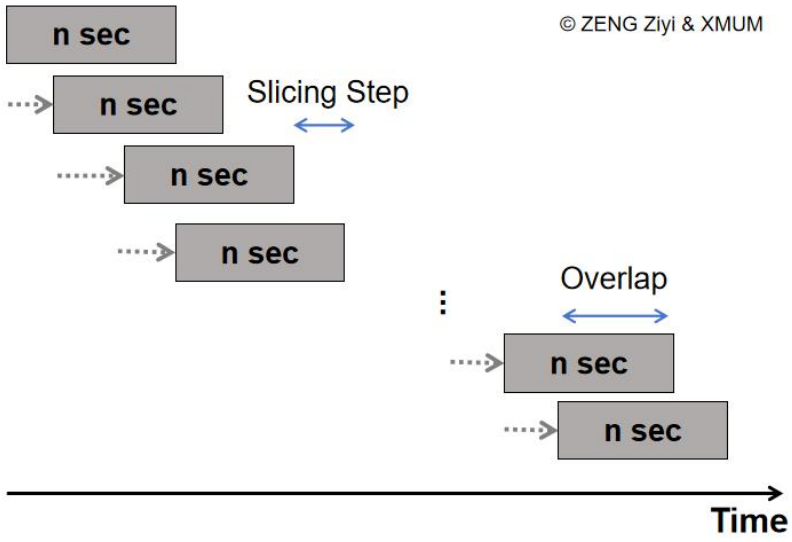

Figure 3.6: Slicing Windows Design. n is the duration of the slicing windows

3.4.2 Optimizer and Learning Rate Scheduler

AdamW is a popular optimizer in model training (Loshchilov & Hutter, 2019). We set the optimizer according to the recommended parameters ($\beta 1 = 0.9$, $\beta 2 = 0.999$, $\varepsilon = 10\text{^-}8$)

For learning rate (LR) scheduler, we used a linear LR scheduler on Convolutional-base FE and Recurrent-base FE. Specifically, the learning rate is set at the beginning of our model training to $1 \times 10^{-4,}$ which is a relatively high value to speed up the initial convergence of the model. We set a gamma value of 0.6, which means that every 5 iterations (with a tuning step of 5), the learning rate decays by a factor of 0.6 of the current one. On Transformer-base FE, however, preliminary experiments demonstrate that the warm up learning rate regulator does not lead to improved model performance, refer to Appendix D. But still, cosine LR scheduler with warmup is employed and warmup step is set to 5.

3.4.3 Loss Function

Currently, in epilepsy-related research species, the binary cross entropy (BCE) loss function has gained a lot of popularity. BCE loss is commonly used in model training for binary classification problems, where the goal is to minimize the cross entropy between the predicted probability distribution and the true label distribution. It has been widely used in epilepsy prediction (Truong et al., 2018; Xu et al., 2020) and detection (Xu et al., 2024). The formula is as follow:

$$BCE\ Loss = -\frac{1}{N}\sum_{n=1}^{N} y_i \cdot log(\overline{y_i}) + (1 - y_i) \cdot log(1 - \overline{y_i}) \quad (1)$$

where y_i is the true(target) label and $\overline{y_i}$ is the predict label.

However, BCE loss struggles to address the issue of class imbalance between positive and negative samples. Although many improvements have been proposed, such as focal loss (Lin et al., 2018), this work opts to follow the mainstream experimental paradigm and continues to use BCE as the loss function for safety reasons.

3.4.4 Early Stopping

Selecting the right number of iterations (epoch) for training a deep learning model is another essential decision. The maximum number of training iterations in this work is 50 epochs. The quantity of training iterations isn't always set in stone, though. The training will end after two consecutive epochs if the validation loss does not decrease. The model's fixed weights will be applied during evaluation. This shortens the training period and keeps the model from becoming overfit.

3.5 Post-processing

When training an algorithm(model) for brain disease like epilepsy, isolated

false-positive (FP) results during the interictal period are frequently encountered. These FP results could result in the "*wrong alarm*" of algorithm. And it will further badly affect patients' treatment choices and day-to-day activities.

In this study, we adopt an approach called k-of-n strategy, to further optimize the accuracy of the prediction, which is proposed by (Truong et al., 2018). k-of-n strategy is based on the idea that the algorithm issues an alert only when there are at least k positive predictions in n consecutive time points. This approach can be regarded as a conservative filtering mechanism because it requires multiple positive predictions in a short period of time. Therefore, it can reduce false alarms due to occasional noise or anomalies.

In this study, we set this two value to 8 and 10, separably, it means the algorithm will only raise an alert if at least 8 sample points in the CHB-MIT database have positive predictions.

3.7 Evaluation Approach

This work uses *five* metrics to evaluate the model. The detail of each metrics is below:

Accuracy (*ACC*), indicates the ratio of the number of correctly classified samples. F1 Score (*F1*), which is the reconciled mean of precision and recall. Area Under the Receiver Operating Characteristic Curve (*AUROC*), which is the area under the ROC curve. Average Precision (*AP*), which is a weighted average of the precision under different thresholds, reflecting the performance of the model under various thresholds. The last two metrics are Sensitivity (*SEN*), indicates the proportion of epilepsy samples correctly detected among all seizures in the specific patient, and the Detection Latency (*Lat*) between the model's alert and the seizure. They are calculated by the following formula:

$$Accuracy(ACC) = \frac{\mathrm{TP} + \mathrm{TN}}{\mathrm{TP} + \mathrm{TN} + \mathrm{FP} + \mathrm{FN}} \times 100 \quad (2)$$

$$F1\ Score(F1) = \frac{2*Precision*Recall}{Precision+Recall} \times 100 \quad (3)$$

$$Average\ Prediction(AP) = \sum(\mathrm{R_n}\text{-}\mathrm{R_{n\text{-}1}})\mathrm{P_n} \quad (4)$$

$$Sensitivity(Sen) = \frac{\text{Seizure Detected/Predicted}}{Total\ Seizure} \quad (5)$$

$$\text{Detection Latency}(Lat) = \text{ Alarm Time} - \text{Seizure Onset Time} \quad (6)$$

Chapter 4: Experimental Result

The experimental results will be shown in detail in this chapter. This chapter is divided into five topics to explore the feature extraction performance of different structures and their comparison in turn. The first three topics (i.e. topic 4.1 to 4.3) show the experimental results of convolutional, Recurrent and transform Feature Extractor (FE) respectively. The performance of each FE and each scale is evaluated by several metrics to ensure the comprehensiveness and accuracy of the comparison. Then, topic 4.3 focuses on the performance of the hybrid feature extractor. The hybrid feature extractor combines the advantages of the first three structures and aims to improve the effectiveness of feature extraction. Finally, the fifth theme will show the experimental results after shortening the sliding window.

All experiments in this study were done on the author's laptop computer. The computer was configured with 32GB of RAM, an NVIDIA RTX 4060 graphics card, and an AMD R9 7940HX processor.

4.1 Performance with Convolution FE

Table 4.1 shows the performance comparison of using different sizes of convolutional Feature Extractor (FE) models. Overall, the large model performed slightly better in detection latency (detection latency) with a mean value of 3.96 seconds, while the small model had a mean detection latency of 4.63 seconds. In the CHB-MIT dataset, there were a total of 100 seizures, and 99 seizures were detected by both models, so the sensitivity (Sensitivity) of both model constructs was 99%.

Individual differences in model performance were evident from a patient-specific perspective. The shortest delay occurred in patient 21 at 1.91 seconds, however the longest delay was still greater than 10 seconds. The large model did not dominate in all patients. In 10 out of 19 patients, the large FE model outperformed the small

model in terms of detection delay. The variance of delay on the small model was 3.21 seconds, which was significantly greater than the variance of delay on the large model of 2.37 seconds.

Particularly interesting is that patient 11 had a detection latency of 12.48 seconds on the small FE model with a variance of 15.79 seconds, whereas on the large model, the detection latency decreased significantly to 4.28 seconds with a variance of 4.49 seconds, a significant difference.

Patient ID	Conv FE(Small)		Conv FE(Large)	
	Lat	*Sen*	*Lat*	*Sen*
1	2.65(2.21)	7/7	**2.36(1.76)**	7/7
2	6.24(4.26)	3/3	**5.93(3.48)**	3/3
3	3.09(2.48)	7/7	**2.82(1.57)**	7/7
4	4.72(3.58)	3/4	**3.80(4.60)**	3/4
5	**4.25(1.61)**	5/5	4.67(1.83)	5/5
6	**2.48(0.13)**	10/10	2.56(0.12)	10/10
7	6.15(2.47)	3/3	**5.27(2.95)**	3/3
8	3.77(2.74)	5/5	**3.69(3.24)**	5/5
9	5.43(4.74)	4/4	**4.75(3.77)**	4/4
10	**2.00(1.32)**	7/7	2.73(2.34)	7/7
11	12.48(15.79)	3/3	**4.28(4.49)**	3/3
14	**4.09(0.86)**	8/8	4.48(1.15)	8/8
17	**5.29(0.75)**	3/3	6.02(1.32)	3/3
18	6.59(5.76)	6/6	**3.83(2.57)**	5/6
19	3.31(0.46)	3/3	**2.33(0.68)**	3/3
20	**3.61(2.47)**	8/8	4.08(2.48)	8/8
21	**1.91(1.84)**	4/4	2.08(1.19)	4/4
22	**6.61(2.71)**	3/3	6.87(3.44)	3/3

23	3.30(4.92)	7/7	**2.73(2.17)**	7/7
Total	4.63(3.21)	99%(99/100)	**3.96(2.37)**	99%(99/100)

Table 4.1: Comparison in Convolution FE Performance with Different Size. Delay: Detection Latency in second. Sensitivity: Ratio in Detected Seizure and All Seizure contained in CHB-MIT database

4.2 Performance with Recurrent Feature Extractor

Patient_id	Rec FE(Small)		Rec FE(Large)	
	Lat	*Sen*	*Lat*	*Sen*
1	**2.70(1.91)**	7/7	3.39(2.11)	7/7
2	6.15(3.37)	3/3	**5.71(3.72)**	3/3
3	3.22(2.75)	7/7	**2.67(1.65)**	7/7
4	4.22(2.76)	3/4	**3.17(3.35)**	3/4
5	3.84(2.71)	5/5	**2.86(1.87)**	5/5
6	**2.30(0.31)**	10/10	2.39(0.28)	10/10
7	5.58(2.89)	3/3	**5.36(3.39)**	3/3
8	**4.59(2.93)**	5/5	5.80(3.50)	5/5
9	3.06(0.90)	4/4	**2.77(1.01)**	4/4
10	3.41(2.47)	7/7	**2.55(1.69)**	7/7
11	**0.93(0.90)**	2/3	1.16(1.14)	2/3
14	5.23(3.63)	8/8	**3.51(1.20)**	8/8
17	5.34(1.86)	3/3	**4.77(2.08)**	3/3
18	3.27(2.92)	5/6	**3.02(2.43)**	5/6
19	4.88(2.74)	3/3	**4.48(2.81)**	3/3
20	**2.92(2.88)**	8/8	3.14(2.66)	8/8
21	2.12(1.28)	4/4	**1.90(1.83)**	4/4
22	**6.85(4.19)**	3/3	8.09(4.17)	3/3
23	3.63(4.17)	7/7	**2.33(1.95)**	7/7

Total	3.91(2.5)	97/100(97%)	**3.83(2.25)**	97/100(97%)

Table 4.2: Comparison in Recurrent FE Performance with Different Size. Delay: Detection Latency in second. Sensitivity: Detected Seizure and All Seizure contained in CHB-MIT database(Ratio); Rec FE: Recurrent Feature Extractor. Format: Mean(Std)

Table 4.2 demonstrates the performance comparison using the Recurrent FE model with different sizes. Both models are identical in the number and distribution of detected epilepsies, which are 97. However, the large model significantly outperforms the small model in terms of detection latency, with average latencies of 3.83 and 3.91 seconds, respectively.

Broken down to the classification of each patient, the small model achieved leading results on the detection of 6 patients, namely patients 1, 6, 8, 11, 20 and 22. Whereas the large model performed better on most of the patients, achieving a lower detection latency. This suggests that in terms of overall performance, the large model has an advantage in reducing detection latency, but on individual patients, the small model still provides better detection results.

4.3 Performance with Transformer Feature Extractor

Table 4.3 shows the performance comparison using different sizes of Transformer Feature Extractor (FE) models. Overall, the large model has a slight advantage in detection latency (detection latency) with a mean value of 3.78 seconds, which is slightly faster compared to the small model's 3.80 seconds. However, the large model only detected 96 seizures, slightly lower than the 97 of the small models.

Patient ID	Transf FE(Small)		Transf FE(Large)	
	Lat	*Sen*	*Lat*	*Sen*
1	2.61(1.74)	7/7	**2.50(1.84)**	7/7
2	8.05(6.58)	3/3	**5.88(4.80)**	3/3

3	**2.92(1.93)**	7/7	2.94(1.98)	7/7
4	**4.74(3.56)**	3/4	4.75(3.59)	3/4
5	4.03(3.55)	5/5	**3.65(3.14)**	5/5
6	**2.55(0.09)**	10/10	2.59(0.35)	10/10
7	**5.36(2.98)**	3/3	5.49(2.84)	3/3
8	3.98(3.54)	5/5	**3.24(3.57)**	4/5
9	4.36(4.77)	4/4	**4.29(4.21)**	4/4
10	**2.35(2.02)**	7/7	2.48(2.17)	7/7
11	**0.89(0.86)**	2/3	0.96(0.94)	2/3
14	3.63(1.48)	8/8	**3.55(1.20)**	8/8
17	**6.24(1.15)**	3/3	6.80(1.00)	3/3
18	5.73(6.51)	5/6	**5.47(6.98)**	5/6
19	**2.80(0.67)**	3/3	2.99(0.67)	3/3
20	**3.33(2.60)**	8/8	3.72(2.45)	8/8
21	**1.85(1.62)**	4/4	2.37(1.47)	4/4
22	**5.27(2.52)**	3/3	6.14(2.52)	3/3
23	**1.66(1.45)**	7/7	2.16(1.74)	7/7
Total	3.80(2.61)	97/100	**3.78(2.49)**	96/100

Table 4.3: Comparison in Transformer FE Performance with Different Size. Latency: Detection Latency in second; Sensitivity: Ratio in Detected Seizure and All Seizure contained in CHB-MIT database; Transf FE: Transformer Feature Extractor. Format: Mean(Std)

From a patient-specific perspective, the small model outperformed the large model in 12 patients with epilepsy, while the large model performed better in 7 patients. Of particular note, for patient #8, the detection latency for the large model was 3.24 seconds, significantly better than the 3.98 seconds for the small model. However, this patient had a total of 5 seizures, and the large model detected only 4, whereas the small model detected all of them. In addition, the large and small models were

identical in terms of missed detections on all patients except for the missed detection on patient number 8.

4.4 Performance with Hybrid FE

In the previous experiments, we have tested and compared the performance of individual feature extractors (FEs) in order to understand the performance of different types of FEs on specific tasks. Based on this, this work further explores the performance of hybrid FEs with a view to improving the overall performance of the model by combining FEs. As selection of two components of hybrid FE, the choice can be the same type (e.g. Conv and Conv) or different (Conv and Rec).

In Section 2.5, the hypothesis of this work is that mixing different FEs helps to improve the performance of the whole model. However, it is not fair to directly compare the hybrid FE with a single FE because the model structure is different between a single FE structure and a hybrid FE (see Figure 3.1a for details). A more effective way is to use two FEs of the same type as components of the hybrid FE (T. Liu et al., 2020), this can work as the baseline in comparison.

Based on the discussion above, as for same type hybrid FE design (called as “Similar hybrid FEs” in Table 4.4), there are various ways to choose the components of hybrid FEs (e.g., Conv-Large & Conv-Large, Transf-L & Transf-S, etc.). However, FEs of the same type with same scale is expected to pass the same feature vectors when reasoning and training, and thus hybrid FEs should not use the same FE as component but similar. Here again, we propose the hypothesis that FEs of different scales can model information at different scales, and mixing the feature vectors output from them can help to obtain feature representations at different scales, which can improve the performance of the whole model. Finally, considering the time factor, we propose only one hybrid FE structure based on the same type of components, namely Conv-Large and Conv-Small.

As for hybrid FE with different component design (or called as “different hybrid FEs” in Table 4.4), however, considering that we have three types of FEs (Conv, Rec, Transf) and two scales for each type (large and small), this implies that there are theoretically 36 different ways of combining them. A complete performance test of these 36 combinations would consume a large amount of GPU computational resources and time, and according to preliminary estimates, as many as 4,500 GPU minutes would be required, which is impractical in practice.

To overcome this challenge, we have carefully selected 4 out of 36 possible combinations of hybrid FE structures that we believe have the most potential to further improve the performance of the model. The choice of component in combination is based on the following considerations:

Recurrent-Large FE as one of the components because it performed best in the single FE experiments. We speculate that combining it with other types of FEs may lead to further performance improvements.

- Transformer-Large and Small FE with the aim of investigating how the performance of transformed FEs varies in a hybrid structure, and the effect of different sizes of FEs on the performance of the hybrid model.
- Convolution FE although is not the best choice in single FE experiments, it may still have unexpected effects in hybrid structures because the convolution operation has unique advantages in processing spatial data.

Taking the above factors into consideration, we finally identified FIVE ways of combining hybrid FEs, which are demonstrated in Table 4.4. These combination ways not only consider the characteristics of different FE types, but also their scales, as well as their performances in single FE experiments. We expect that these well-designed combinations can significantly improve the performance of the model while maintaining a reasonable use of computational resources.

	Feature Extractor		Parameters			Training Time
	A	B	A	B	Total	
Similar	Convolution FE (Large)		14M	14M	28M	131.2 min
Different	Convolution FE (Large)	Transformer (Large)	14M	50M	64M	300.0 min
	Convolution FE (Large)	Transformer (Small)	14M	23M	37M	173.4 min
	Recurrent FE (Small)	Transformer (Small)	1M	23M	24M	112.5 min
	Recurrent FE (Large)	Transformer (Small)	7M	23M	30M	140.6 min

Table 4.4: Components in Hybrid Network

In this study, we conduct a comprehensive side-by-side comparison of the performance of the proposed fusion feature extractor (FE). Specific details of the comparison and data analysis can be found in Appendix A3. After comprehensively comparing different hybrid FE structures, the hybrid FE combining a Conv-Large and a Transf-Large FE achieves the highest results in all performance metrics. This best hybrid FE achieves an excellent detection latency of 3.72 seconds and a high latency consistency of 97%.

To further validate the performance of this hybrid FE, we conducted a comprehensive evaluation, and all the performance metrics are shown in detail in Table 4.5. These metrics include, but are not limited to, accuracy, recall, F1 score, and detection latency, which together provide us with a comprehensive view of the hybrid FE performance.

Patient ID	Lat	Sen	Acc	F1	AP	BCE
1	2.59(2.07)	7/7	1.00(0.01)	0.99(0.01)	1.00(0.01)	0.03(0.05)
2	6.43(4.06)	3/3	0.87(0.16)	0.81(0.26)	0.93(0.10)	0.41(0.50)
3	2.88(1.73)	7/7	1.00(0.00)	1.00(0.00)	1.00(0.00)	0.01(0.01)
4	5.33(4.04)	3/4	0.86(0.21)	0.73(0.42)	0.85(0.22)	1.22(1.86)
5	4.18(2.43)	5/5	0.99(0.01)	0.99(0.01)	1.00(0.00)	0.03(0.03)

6	2.42(0.21)	10/10	1.00(0.01)	1.00(0.01)	1.00(0.00)	0.01(0.01)
7	3.65(0.32)	3/3	0.93(0.07)	0.92(0.08)	0.95(0.06)	0.33(0.39)
8	3.43(3.27)	5/5	0.96(0.04)	0.96(0.05)	0.97(0.04)	0.23(0.32)
9	5.20(4.70)	4/4	0.97(0.03)	0.97(0.03)	1.00(0.00)	0.07(0.08)
10	1.96(1.68)	7/7	1.00(0.01)	1.00(0.01)	1.00(0.01)	0.03(0.05)
11	0.02(0.0)	2/3	0.81(0.21)	0.85(0.16)	0.98(0.02)	0.54(0.52)
14	4.75(1.07)	8/8	0.97(0.04)	0.96(0.05)	0.99(0.02)	0.12(0.14)
17	5.17(0.62)	3/3	0.95(0.01)	0.94(0.01)	0.98(0.01)	0.16(0.03)
18	4.09(3.39)	5/6	0.86(0.14)	0.79(0.23)	0.95(0.07)	0.43(0.41)
19	2.73(0.70)	3/3	1.00(0.01)	1.00(0.00)	1.00(0.00)	0.01(0.01)
20	4.07(2.23)	8/8	0.98(0.02)	0.98(0.03)	0.99(0.02)	0.07(0.08)
21	2.57(1.88)	4/4	0.98(0.01)	0.98(0.02)	1.00(0.00)	0.06(0.04)
22	6.40(3.38)	3/3	0.99(0.01)	0.99(0.01)	1.00(0.00)	0.02(0.01)
23	2.97(2.37)	7/7	0.95(0.09)	0.93(0.14)	0.99(0.02)	0.14(0.19)
Total	**3.72(2.11)**	**97/100**	**0.95(0.09)**	**0.93(0.14)**	**0.99(0.02)**	**0.20(0.24)**

Table 4.5: Performance of Hybrid Network with Convolution FE and Transformer FE. Lat: Detection Latency; Sen: Sensitivity; Acc: Accuracy; F1: F1-Score; AP:Average Precision; BCE: Binary Cross Entropy loss. Format: Mean(Std)

4.5 Performance with Short windows Size

In the previous chapters, the optimal hybrid FE structure was selected and tested. In this chapter, the sliding window of the model will be adjusted from a length of 5 seconds to 2 seconds. The model's structure and other experimental details will remain unchanged. Subsequently, this study will assess whether the detection latency of the model have changed with the length of windows.

Table 4.6 presents the model's performance using the 2-second sliding window and compares it to the performance with the 5-second sliding window. Unexpectedly, the model's performance improved significantly with the 2-second sliding window. On average, the detection delay of the model using the 2-second sliding window was 1.83 seconds, which is notably faster than the 3.72 seconds with the 5-second window. This represents an overall improvement in detection delay speed of approximately 49.19%. Out of 19 patients, patients 18 showed significant performance enhancement with the 2-second sliding window. Patient 22 exhibited

the most remarkable improvement, with the detection delay decreasing by 3.96 seconds. However, the delay for patient 11 increased by 1.39 seconds.

Patient ID	*Lat*	*Improvement*	*Sen*
1	1.09(0.94)	**-1.5**	7/7
2	3.42(2.47)	**-3.01**	3/3
3	1.04(0.65)	**-1.84**	7/7
4	2.86(3.50)	**-2.47**	3/4
5	2.10(2.30)	**-2.08**	5/5
6	1.11(0.28)	**-1.31**	10/10
7	1.70(0.27)	**-1.95**	3/3
8	2.56(2.83)	**-0.87**	5/5
9	1.29(0.86)	**-3.91**	4/4
10	0.83(0.78)	**-1.13**	7/7
11	1.41(1.38)	**+1.39**	3/3
14	2.35(0.61)	**-2.4**	8/8
17	4.12(0.81)	**-1.05**	3/3
18	3.09(4.02)	**-1.00**	5/6
19	0.56(0.44)	**-2.17**	3/3
20	2.29(1.88)	**-1.78**	8/8
21	0.48(0.39)	**-2.29**	4/4
22	2.44(1.91)	**-3.96**	3/3
23	0.17(0.25)	**-2.8**	7/7
Total	**1.83(1.39)**	**-1.89**	**97/100**

Table 4.6: Performance of Hybird Network with shorter slicing windows(2 seconds).Lat: Detection Latency; Sen: Sensitivity; Acc: Accuracy; F1: F1-Score; AP:Average Precision; BCE: Binary Cross Entropy loss. Format: Mean(Std)

Chapter 5: Discussion

The experimental results in Chapter 4 are discussed in detail in this chapter, which includes 5.1 discussing the impact of the size of the FE on the detection delay, 5.2 exploring the improvement of the model performance by hybrid FEs, 5.3 discussing the choice of FEs in resource-constrained scenarios, and 5.4 analysing the impact of a shorter sliding window on the model. Except for 5.3, each topic in this chapter corresponds to one of the hypotheses presented in Chapter 2, Section 2.5, respectively. Readers are advised to complete Chapters 3 and 4 before reading this chapter.

5.1 Feature Extractor Size

To comprehensively and objectively investigate the effect of Feature Extractor (FE) size on model performance, it is useful to study multiple perspectives.

The performance of three types of Feature Extractors (FEs) at two different scales is displayed in Figure 5.1a. The Convolution-Large FE obtains an advantage on 11 out of 21 patients, while the latency at large scale (3.96) is numerically smaller than that at small scale (4.63), which suggests that the convolutional FE performs better at large scale in terms of latency. Like Convolution FE, Recurrent's large-scale FE achieved an advantage on 13 out of 21 patients. Numerically, the latency of the large FE (3.93 seconds) is similarly smaller than that of the small FE (3.83 seconds), suggesting that the Recurrent FE would be expected to have a small performance gain with increasing size. However, the opposite is true for Transformer. Its large-scale FE achieves an advantage with only 7 patients.

Figure 5.1b further demonstrates the performance comparison between FEs of different sizes, where independent t-tests were employed. The p-values for the three types of FE are 0.30, 0.61, and 0.97. The p-value for the Convolution FE is the

smallest, indicating that an increase in FE size provides the greatest performance gain for the Convolution FE. However, for all types of FE, the difference in performance between the two groups is not significant. Figure 5.1c compares the performance of the different sizes of FE on a per-patient basis, and further shows that for all three types of FE, the difference in performance between the two sizes does exist but is not significant. This "non-significant performance improvement" proves in another way that the current progress in algorithmic detection latency is limited to the model structure rather than the model scale. Making the size of the FE larger only improves the performance of the model in a small way and does not bring fundamental advances to the model.

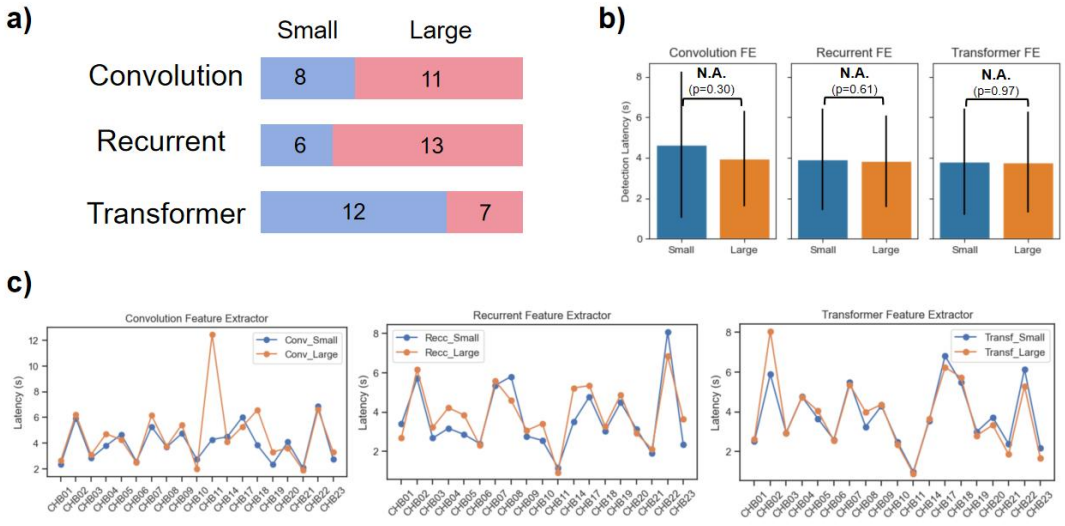

Figure 5.1: Comparison of different size FE performance. a) Win lose chart of FE performance; b) Bar chart of FE performance;c) Line chart comparison with each patient. Error bar: standard deviation, N.A.: no significant different between two group.

The anomalous performance of the Transformer FE deserves to be discussed. There is no direct relationship between FE size and its performance. We speculate that this may be related to the high requirement of the Transformer structure on the number of samples. Compared to the other two structures, Transformer inherently requires a

huge sample size for a perfect fit. This has been confirmed in the field of computer vision (Dosovitskiy et al., 2020). In our experiments, it is likely that two scales of transformer are under-fitting states. For model training with small sample sizes, large transformers do not necessarily give good results. This phenomenon will be further discussed later.

However, the independent samples t-test, as a parametric test method used before, is based on an important assumption that the data for the test should obey a normal distribution. To ensure the accuracy and reliability of the test results, we need to first confirm whether the data comply with this key assumption. For this purpose, we used Quantile-Quantile (Q-Q) plots to visually assess the normality of the data. Figure 5.2 illustrates the Q-Q plots for six different sizes of FE detection delays. As can be seen from the plot, all the data points closely fit on the diagonal line, which indicates that the detection latencies of these FEs are approximately normally distributed, thus fulfilling the assumption condition for performing an independent samples t-test.

It is worth noting that the data points of the large FEs deviate from the ideal diagonal to some extent as compared to the small FEs. This implies that although the detection latency of the large FE remains close to normal distribution, its distribution may have higher dispersion and skewness.

As shown in figure 5.2, the data points of the large-scale FE were more off-diagonal, suggesting that the distribution of their detection latencies may have fluctuated more, which may have led to a decrease in the stability of the model and made the results of the detection latencies more unpredictable. It is speculated that this phenomenon may be related to the insufficient number of training samples in the experiments. CHB-MIT is not a large dataset, and the number of fitting samples for each model training is about two thousand(2K). For a large-scale model, these samples may not be sufficient to fully learn the EEG feature representations of each patient, leading to a certain degree of underfitting. However, the exact reason for this needs to be

further researched and explored by future generations.

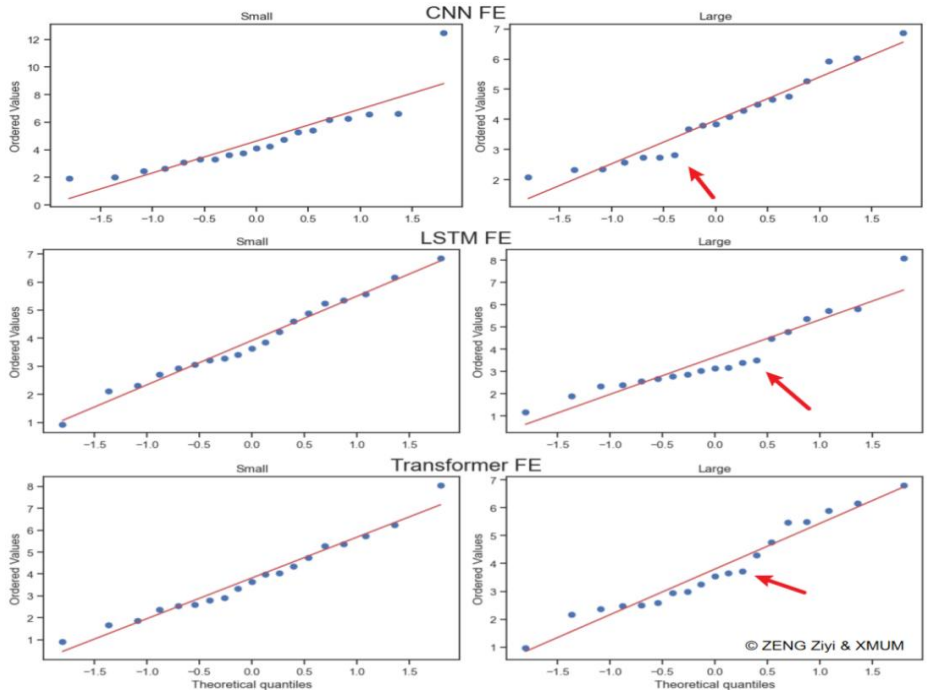

Figure 5.2: Quantile-Quantile Chart of Each Feature Extractor with Different Scale

5.2 Hybrid Feature Extractor

A comprehensive comparison of the detection latency of all the feature extractors (FEs) proposed in this work are shown in Figure 5.3. Overall, three of the five hybrid FE structures proposed in this work approach or exceed the performance of the best single FE. It should be noted that there are still two hybrid FEs with lower performance than the single FE, indicating that the choice of combinations of hybrid FEs still needs to be careful. The detection latency of the best hybrid FE is 3.72 s, while that of the best single FE is 3.78 s, which is 0.06 s slower. Interestingly, the best individual FE is Transformer-Large, which coincidentally is also a component of the best hybrid FE.

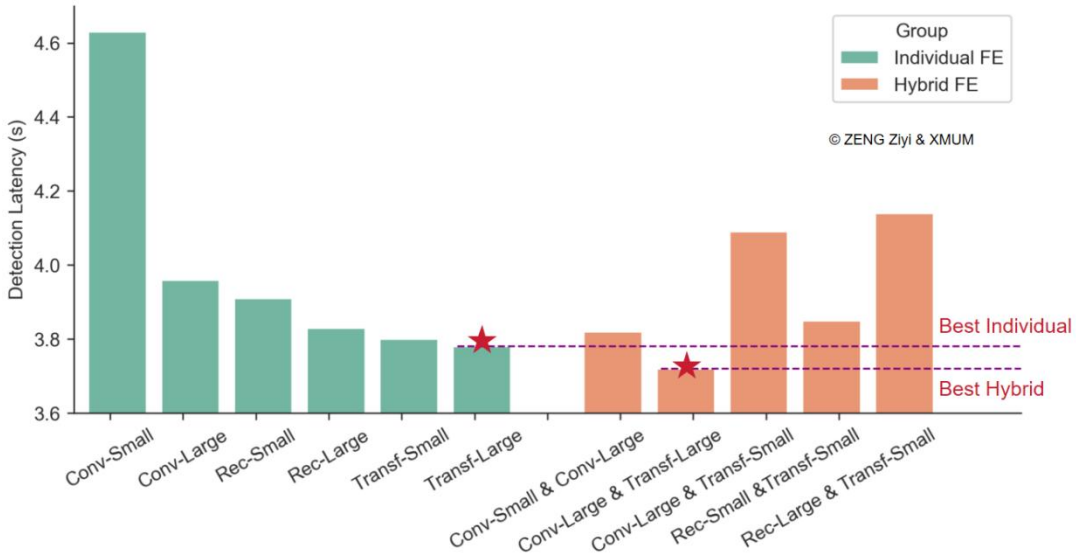

Figure 5.3: Comparison in Detection Latency of All Proposed Feature Extractor

The performance of the individual large-scale convolutional FE is poor from the point of view of the convolutional structure, but when it is combined with the Transformer FE, the latency is faster by 0.24 seconds. This is a good proof of the complementary nature of the convolutional and attention mechanism structures. Specifically, convolutional FE may be able to efficiently extract local features, while Transformer FE excels at capturing global dependencies. This complementarity may result in the hybrid model performing well when dealing with complex tasks, even if one of the convolutional FE structures performs poorly when used independently. This demonstrates that in the hybrid FE structure, different types of FEs can complement each other and combine their respective strengths. This network structure is indeed conducive to improving model performance, in line with the hypothesis of this work.

In addition, the hybrid network in this work uses a parallel FE framework, in which the Convolutional FE and Transformer FE reason separately to generate their respective feature representations, which are finally handed over to a unified common module for computation (see Fig. 3.1a for details). Another combination approach is to place the convolutional layer before the Transformer encoder, which has been validated as effective in epilepsy prediction tasks (Hu et al., 2023). This combination approach was not tested in this work and requires further research.

However, the poorer performance based on the Recurrent and Transformer hybrid FEs is worth discussing. It is speculated that this is more similar to the Transformer structure, both of which are good at modelling global information, which could explain the lack of significant improvement after fusion. In addition, the recurrent structure is less computationally efficient, making it difficult to parallelize the computation, leading to slower training. Therefore, the Loop structure is more suitable for single FE scenarios rather than the best choice for hybrid networks.

5.4 Windows Size

This study provides insight into the effect of sliding window length on model performance. The experimental data show that when the sliding window length is shortened to 2 seconds, the average detection delay is significantly reduced from 3.72 seconds to 1.83 seconds. This result suggests that shortening the sliding window helps to improve the model performance. Specific details are shown in Figure 5.3, which demonstrates the comparison of latency based on different sliding window lengths, detailing the latency performance of each patient with different sliding windows. With the exception of patient 11, all patients have significantly lower latency, indicating that this phenomenon is generalisable in most patient cases.

Additionally, a study from Stanford University noted that shortening the sliding

window can modestly improve the model's F1 score and AUROC performance. However, there are no studies that have explored the relationship between sliding window length and detection latency. We hypothesized that this is because the metric of detection latency is often overlooked in related studies. Therefore, this study demonstrates for the first time that a shorter time window helps to optimize the detection delay time of the model.

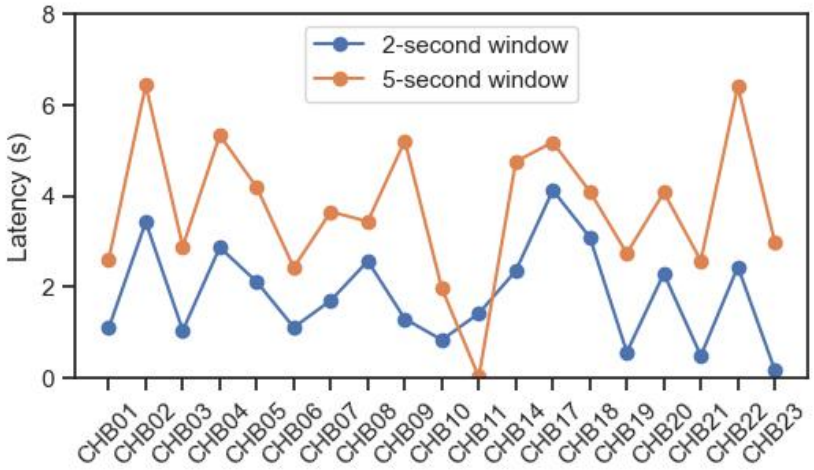

Figure 5.3: Comparison in Detection Latency of All Proposed Feature Extractor

A positive correlation between time window length and detection latency was observed in this experiment. It is hypothesized that a shorter time window reduces data noise and is more conducive to model fitting and detection. However, the specific details of this mechanism still need to be further investigated to clarify the actual path and mechanism of the effect of time window length on model performance improvement. With these preliminary findings, this study provides new ideas and directions for future related research.

5.5 Real Use Case Comparison

In practical applications, arithmetic resources are always limited, and the performance of models in many cases is constrained by hardware resources. Therefore, it becomes crucial to train models with better performance under limited resources. In other words, if a model has fewer parameters and at the same time has a shorter detection delay, the better the performance of the model. Therefore, to quantify the performance of a model with a limited number of parameters, this work proposes the following formula to evaluate the potential of the model:

$$Capacity(CAP) = \text{Params} \times e^{\beta * \text{Lat}} \times \alpha \quad (1 < \text{Lat} < 5) \tag{7}$$

Where, Params is the total number of parameters of the model, Lat is the detection delay time, α and β is the scaling factor. This formula was chosen to be able to balance the change in parameters with the change in latency. The lowest in capacity means the better FE under the computing resource-limited environments. In this study, we choose $\alpha = \frac{1}{10^{14}}, \beta = 4$. These two hyper-parameters are derived from fitting two data points (i.e. Conv FE-Small and Conv FE-Large) to the formula 7.

Table 5.1 shows all the FE's. From it, it can be learned that Recurrent FE-small obtains the best value as 2.5 in individual group. This highlights the discussion above the the benefit of Recurrent structure as it serves as individual FE. For hybrid group, Conv-Large FE(Large&Small) yielded the lowest result, this proved uncovered potential of hybrid structure with same component, although it is not the best hybrid FEs in previous experiment. However, it still needs to be carefully selected according to the actual situation in practical applications.

There is an interesting finding in the capacity of 2 second hybrid FE. It achieves 0.0015, which is the best one among all proposed FEs. This means that this hybrid

FEs under 2 second slicing windows can give the best performance per unit parameter count, i.e., the shortest latency is achieved. Again, there is no published work to study the potential of the shorter slicing windows in the relation of latency, thus the conclusion of these should under concern.

	Feature Extractor		Parameters	Latency	Capacity
Individual	Convolution FE	Small	0.8M	4.63	3.0
		Large	14M	3.96	3.0
	Recurrent FE	Small	1M	3.91	**1.78**
		Large	7M	3.83	8.8
	Transformer FE	Small	23M	3.80	2.5
		Large	50M	3.78	5.1
Hybrid	Convolution FE (Small)	Convolution FE (Large)	28M	3.82s	**3.3**
	Convolution FE (Large)	Transformer (Large)	64M	3.72s	5.0
	Convolution FE (Large)	Transformer (Small)	37M	4.09s	14.2
	Recurrent FE (Small)	Transformer (Small)	24M	3.85s	3.3
	Recurrent FE (Large)	Transformer (Small)	30M	4.14s	14.2
Hybrid (2s)	Convolution FE (Large)	Transformer (Large)	64M	1.83s	**0.0015**

Table 5.1: Capacity of all Feature Extractors

5.6 Comparison with Other Works

The main experimental results of this study are based on the completion of a 5-second sliding window, where the individual feature extractors (FEs) and the hybrid FE achieved a detection delay of 3.78 seconds and 3.72 seconds, respectively. Table 5.2 demonstrates the comparison of this study with other studies. The latency

detection results of this study have proved to be ahead of the results of most of the peers.

The model structure of this study is improved upon the state-of-the-art structures proposed by other studies, which have been shown to achieve results close to the state-of-the-art (SOTA) in their respective tasks, i.e., epilepsy prediction (Truong et al., 2018), seizure classification (T. Liu et al., 2020),computer vision (Dosovitskiy et al., 2020). The present study migrated and optimized these structures for epilepsy detection, so obtaining leading-edge results was expected.

However, the detection delay in this experiment is still about 1.5 seconds longer than Xu's work. We speculate that this may be due to inconsistency in the decision rule. This study used a traditional decision rule, the k of n rule, which states that the algorithm alerts if more than k of the n samples exceed the threshold. In contrast, Xu's work used the rectified predictive ictal probability (RPIP) to decrease detection latency and false detection rate (FDR), which is an improvement on the traditional decision rule (Xu et al., 2024). Due to practical complexities and time constraints, this RPIP method could not be used in this study, which may explain the poorer results in this study.

The detection delay performed satisfactorily under a 2-second sliding window. Based on our current knowledge, this is the lowest detection latency in the field of epilepsy detection, in other words, the result has become the new SOTA. However, due to time constraints, we have not been able to determine whether the 2-second sliding window is the most favorable choice for detection latency or whether other metrics become worse under this window length. Therefore, more experiments and studies are needed to further validate these results.

Ref	EEG Form	Feature Extractor	LOSOCV	Hybrid Network	Windows Size	Lat	Sen

(A. H. Shoeb & Guttag, 2010)	Frequency-domain	SVM	✓	-	6s	4.6s	96%
(L. Vidyaratne et al., 2016)	Raw	-	-	-	1s	7s	100%
(Hossain et al., 2019)[$]	Raw	2D-CNN	-	-	2s	-	90%
(Burrello et al., 2021)[$$]	Statistical	1D-CNN	-	✓	2s	8.8s	97.7%
(C. Li et al., 2021)	Statistical+ EMD	SVM	-	-	4s		93.6%
(X. Wang et al., 2021)	Raw	1D-CNN	-	-	2s	8.1	99.3%
(Shen et al., 2022)	Spectrogram	RUSBoosted	-	-	30s	10.4s	96.1%
(Shen et al., 2023)	Spectrogram	2D-CNN	-	-	5s	10.5s	98.9%
(Cimr et al., 2023)	Raw	2D-CNN	-	-	23.6s	-	98.5%
(Xu et al., 2024)[$$$]	Spectrogram	3D-CNN	✓	-	5s	2.3s	95.0%
This work	Spectrogram	Transformer	✓	-	5s	3.80s	
		Transformer &CNN	✓	✓	5s	3.72s	97%
		Transformer &CNN	✓	✓	2s	**1.83s**	

Table 5.2: Comparison to Other Work. $: the result is validate on cross-patient. $$: the result is validate on SWEC-ETHZ dataset. $$$: the result is validate on non-K-of-n decision rule

5.7 Limitation of Work

There are several limitations of this study:

Firstly, detection delay was chosen as the main basis for optimising and evaluating the model in this study. This resulted in other important metrics being ignored to varying degrees. For example, although false detection rate (FDR) is a key metric, it was not measured in this study due to time constraints. We found that to measure the FDR would extend the model evaluation time by at least a factor of two, which

requires a significant investment of computational resources and time.

Second, the excellent model performance obtained in this study under a 2-second sliding window is only a preliminary result. We found that the detection delay under this window length was significantly reduced to a new level of SOTA. However, due to the lack of supporting data from other peer work, we are unable to determine the validity of these results in a broader range of applications. In order to further validate the effectiveness of the 2-second sliding window, a large number of ablation experiments need to be performed. These experiments should include comparing the performance of different window lengths, different datasets and different feature extraction methods to fully assess the robustness of the model. In addition, the performance of the model in real-world applications, such as its adaptability to different patients and different seizure types, needs to be further investigated and validated.

Furthermore, to ensure the implementability of the proposed algorithm, the concept and formula of *capacity* are introduced in this study. Although we logically justify it, we did not demonstrate the validity of Eq. 7 through rigorous experiments. In the selection of hyperparameters, only the simplest double-digit stronghold fitting method is used to determine them in this study. In fact, more rigorous mathematical derivations and experiments are needed to verify the reasonableness of these choices.

Finally, this study validated the effectiveness of the algorithm only on each individual patient but did not propose and validate a cross-patient model of the algorithm. From some perspectives, this approach is inefficient and unreasonable. The cross-patient epilepsy detection model is close to a large language model in terms of the number of parameters, and its training requires a large number of arithmetic resources, which is why it could not be attempted in this study.

Therefore, this study achieved leading results in some respects, but further

experiments and research are needed to compensate for the above limitations and ensure the comprehensiveness and reliability of the results.

Chapter 6: NeuroSafe- A Close-loop Real Time Neuroimaging Monitoring System(C-RNMS)

The previous chapter has discussed the automated epilepsy detection algorithms to support doctors' diagnosis, and the difficulties doctors have with epilepsy recognition are expected to be addressed. However, we must not lose sight of those patients themselves who play role in epilepsy management, and it is equally important to improve the patient's experience in treatment. In this chapter, a close-loop neuroimaging system is proposed for better serving patient's need in understanding the epilepsy and seizure, with discussed below.

6.1 Introduction to Proposed System

Real-Time Neuroimaging Monitoring System (RNMS) is a state-of-the-art technology for immediate observation and analysis of brain activity. By combining neuroimaging techniques (e.g., functional magnetic resonance imaging and near-infrared spectroscopy) with advanced data processing methods, these systems can capture, analyze, and respond to functional changes in the brain in real-time. The importance of RNMS is unquestionable and has been widely used in specialized healthcare facilities. It has important applications in intraoperative monitoring, epilepsy detection, and brain injury rehabilitation.

However, the current RNMS has several limitations. Firstly, due to the specialized nature of RNMS, only professional healthcare workers can understand and use it, while it is difficult for patients to understand the complex meanings in neuroimaging. Second, remote monitoring solutions are not yet mature, thus most of the current RNMS rely on cable transmission, which limits the convenience and flexibility of remote applications. In addition, existing mature RNMS mostly rely on software on the computer side for real-time local detection, and mobile applications are not yet

mature, limiting the possibility of monitoring anytime, anywhere.

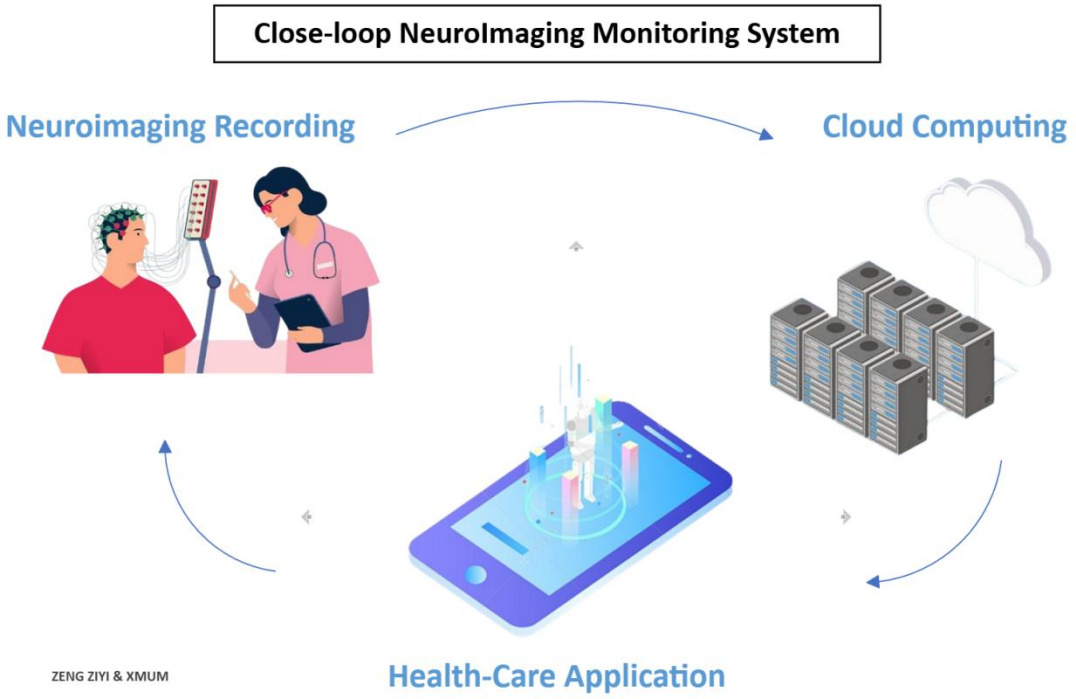

Figure 6.1: Proposed Close-Loop NeuroImaging Monitoring System

To overcome these drawbacks, the convenience of the system can be achieved by introducing Internet of Things (IoT) technologies and remote monitoring solutions, and lowering the threshold for doctors and patients to access information on disease conditions. Therefore, this work proposes a Closed-loop Real-time Neuroimaging Monitoring System(C-RNMS) based on a mobile application, which consists of three components, namely a neuroimaging acquisition system, an artificial intelligence cloud computing platform and a mobile health application.

The neuroimaging acquisition system is responsible for acquiring human brain signals (e.g., EEG, MRI). The system can use the existing proven acquisition equipment in the hospital, such as instruments already in use in hospitals. In this way, there is no need to replace existing brain signal acquisition devices, thus saving costs and simplifying operations. At the same time, the acquisition devices can also be

customized to fit specific scenarios to better meet user needs. For example, portable brainwave acquisition systems can facilitate patients to monitor their brainwave activities at any time in their daily lives. The implementation of the acquisition terminal used in this work is based on a customized solution that not only improves the comfort and convenience of the device, but also ensures the accuracy and reliability of data acquisition.

Cloud computing systems typically include a back-end program for receiving and processing acquired brain signals in real time. Artificial intelligence algorithms can be built into the back-end program to detect the presence of abnormalities such as epilepsy in the brain signals. Once the processing is complete, the back-end program e sends the processed data in chunks to the user's mobile device and displays it in the application.

The mobile health application(m-Health) is the main interface through which the patient interacts with the system. The app contains several features required by epilepsy patients, one of the key features being real-time monitoring of brain signals. The user can view the brain signals in real time on the mobile phone while the AI's predictions are displayed. For instance, if the AI detects a potential seizure, the app immediately alerts the user and provides advice on how to respond accordingly. In addition, the application provides many other features that will be described in detail in Section 6.2.

In a subsequent manuscript, this work will build and run a demonstration of a working R using EEG for brain signals. This system is named NeuroSafe, symbolizing the sense of safety and health that the use of this system can bring to people with epilepsy. With this complete system, we aim to make neuroimaging monitoring more convenient and user-friendly for the benefit of both healthcare professionals and patients. As the three main components of NeuroSafe, the

neuroimaging acquisition system will be described in detail in Section 6.2 and the mobile application will be presented in Section 6.3.

6.2 Brain Signal Acquisition System Hardware Design

As a component of a closed-loop monitoring system, existing brain signal acquisition devices are often bulky and expensive. To this end, this work proposes and implements a simple and low-cost EEG acquisition system built on an Arduino board. Arduino can be understood as a microcomputer, which is the information hub of the IOT. In the proposed system, Arduino is responsible for formatting the received electrical signals and forwarding them to the connected computer through a serial port.

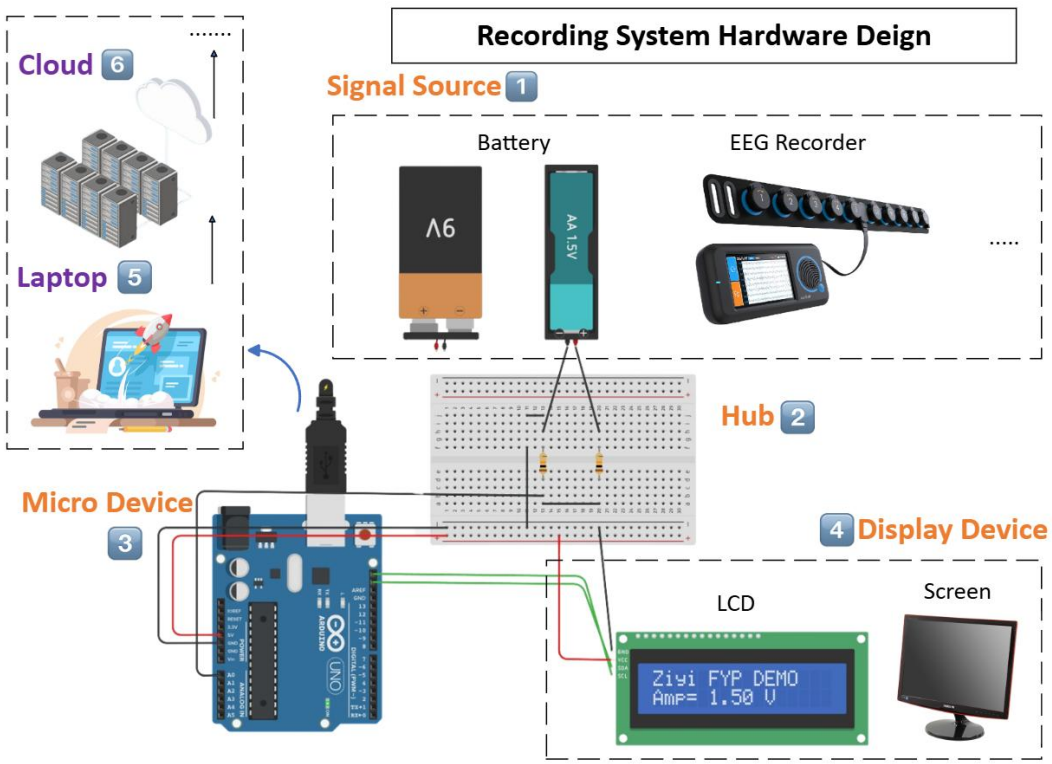

Figure 6.2: Hardware Design of Neuro-imaging Monitoring System

Figure 6.2 shows the schematic of the system implementation, which contains the flow of EEG signals. The EEG signals start at a signal source (part 1), which is

essentially an electrical signal; the signal source can be an EEG recorder (Kamousi et al., 2019) or a simple battery can be used instead. The source sends the EEG signal to the Hub (part 2), which forwards the signal to the Arduino (part 3) according to a predefined circuit setup. the Arduino processes the current signal and transmits it to the embedded display device for display (part 4), and at the same time writes the data to the serial port. The laptop receives the data from the serial port (part 5) and subsequently forwards the data in real time to the cloud server (part 6). The cloud server calculates the data using a series of algorithms and transmits the results to the mobile application for display (not shown in figure).

6.2 Laptop and Cloud Server Program Design

The electrical signals cannot be sent directly from the hardware platform to the server, hence the need for the Neurosafe laptop program running on a Windows system to act as a relay station. To achieve this, this work designed and developed a simple application to read the input signals from the hardware platform, process them and then forward them to the server. A screenshot of the Neurosafe application in action is shown in Figure 6.3, demonstrating the user interface and functionality of the application.

Neurosafe is designed to maximize the user's initiative and therefore gives the user the right to choose the form of the signal in the software. The user can select EEG data (real data) from the hardware platform, which provides real-time and accurate biofeedback data, or in the event that the hardware platform is unavailable, the user can select fake data automatically generated by the software instead for testing and demonstration purposes. The software provides three types of pseudo-data, namely linear wave, sin wave, and EEG wave, where the linear wave represents a simple linear waveform, the sin wave is a sinusoidal waveform, and the EEG wave adopts the data of the first EEG channel of Patient No. 1 in the CHB-MIT database, which

can be pre-processed to simulate real EEG signals. After user click “start” button, laptop program will generate (or fetch from hardware) the corresponding real-time signals, then compress each 0.5 seconds signal (10 data point) into a string. The data block will be stored in the Redis and waiting for mobile application to fetch.

As selection of server, a lightweight application server from Tencent Cloud was chosen, which deployed in Shenzhen, China. The server runs a Docker image of Redis as an efficient in-memory database, which is specially used for staging and forwarding data between the collection end and the mobile end. Redis is known for its fast response capability and high throughput, which is ideal for application scenarios that require real-time data transfer. The server manages and transfers EEG data through Redis, ensuring that the data can be transferred quickly and stably from the collection side to the mobile side, providing users with a smooth experience.

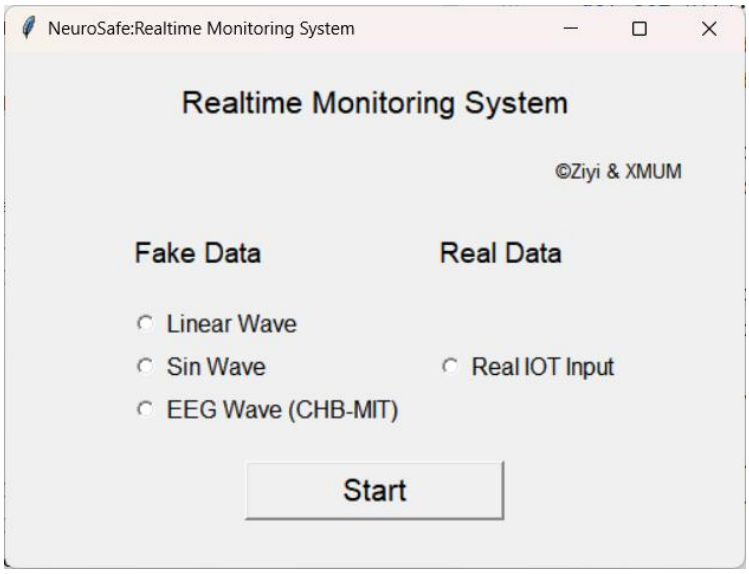

Figure 6.3: Screenshot of NeuroSafe Laptop Program

6.3 Mobile Application Design

6.3.1 Background of Patient Needs

Although epilepsy patients represent only 1% of the global population (Xu et al., 2024), their health needs and health management are equally important. Patients have many specific needs in their treatment, and meeting these specifics requires professional support. Firstly, patients with epilepsy often need to monitor and manage their seizures, including their frequency, duration and possible triggers. Each seizure has its own unique characteristics, so complete records are vital for doctors to get a more accurate picture of the condition. These records can help doctors identify patterns of seizures and potential triggers, providing an important reference for developing a more effective treatment plan. Secondly, patients usually need to take antiepileptic drugs for a long period of time to prevent seizures, and the consequences of forgetting to take the drugs are incalculable. Although self-reminders are the best way to do this, patients often tend to forget. This is especially true for older patients. Therefore, they often need outside support to ensure that medication is taken on time and to avoid missing or repeating doses to ensure that treatment is effective.

Furthermore, patients with epilepsy usually require dedicated care during acute seizures to ensure their safety (Khuda & Aljaafari, 2018). However, due to the uncertainty of seizures, inadequate care may occur. In emergency situations, it is crucial to ensure that patients' cries for help are responded to in a timely manner. Meanwhile, emergency physicians need to be trained accordingly to adopt first aid protocols for different epilepsy types (Urrestarazu et al., 2008). In addition to this, patients with epilepsy need to learn about epilepsy to fully understand their condition. By knowing this information, patients can better manage their condition and work with their doctors to develop the best treatment plan.

Finally, effective communication between patients and doctors is crucial. This ensures that the doctor has a deeper understanding of the patient's condition and needs and provides them with a personalized treatment plan. Patients should fully express their symptoms and feelings so that doctors can make accurate diagnoses and treatment recommendations.

Based on the discussion above, a specially designed app is necessary. Mobile apps are fully portable and are the best choice for patients. Mobile health apps have several features that have great potential to help in the treatment of chronic diseases such as epilepsy (Alzamanan et al., 2021). By recording and analysing data, patients can get a clearer picture of their health and can share it with their healthcare team to better manage their condition.

6.3.2 Market Analysis

There are many mobile applications in the market designed for epilepsy-care. In this section, we aim to explore the strengths and weaknesses of these apps, for the better development of mobile applications in later phases.

First, our study performed an application search in the Google Play Store. More specifically, we used "epilepsy" as a keyword for searching the applications available. Second, we filter the search result based on the following criteria: available in English, free to download in the store, downloaded more than 10,000 times, and designed for people with epilepsy. This strategy was improved from the work of (Alzamanan et al., 2021). The reason why we applied this improved screening strategy is to consider that this study was limited to *smaller scope* and that *Android* is the dominant mobile operating system on phone. Lastly, we selected the top-5 mobile apps, which were Epilepsy Journal, Seizure Tracker, Epistemic App, Helpilepsy, and Epsy.

In this study, we proposed *five* functions to analyze the included mobile apps listed above, which are epilepsy tracking, medication reminders, contacting doctors, knowledge sharing and real-time recording.

Among these features, the *Seizure Tracking* feature allows patients to record and view key information about each seizure. The medication reminder feature automatically reminds patients to take their medication at the prescribed time, helping them to maintain a regular treatment regimen. The *Contact Doctor* feature facilitates communication between doctor and patient, enabling patients to easily book appointments or send epilepsy reports to their doctors. The *Knowledge Sharing* feature teaches patients about epilepsy through specially designed modules to enhance their understanding and management of the condition. The real-time neurological recording feature, on the other hand, is synchronized with neuroimaging devices to visualize and display real-time neuroimaging data (e.g. EEG segments) to patients.

Table 6.1 shows in detail the features supported by each application. All the software had basic epilepsy tracking functionality but differed in other features. In terms of medication reminders, three of the five software programs offer this feature. Except for Seizure Tracker, all the applications included the ability to contact a doctor. For example, Epistemic App can send epilepsy records to a designated doctor in the form of a medical report.

In terms of knowledge sharing, only Epilepsy Journal and Epsy offer epilepsy knowledge dissemination, and this two application include the most comprehensive feature set. The main difference between these two applications is in the visual design, with Epilepsy Journal's interface adopting a more traditional design style. The main difference between the two applicationis in the visual aspect, with Epilepsy Journal having a more traditional interface.

App Name	Fundamental Functionality		Extended functionality			
	Seizure tracking	Medication reminder	Doctor Connection	Knowledge Sharing	Realtime Neuro-Monitoring	News
Epilepsy Journal	✓	✓	✓	✓	-	-
Seizure Tracker	✓	-	-	-	-	-
Epistemic App	✓	✓	✓	-	-	-
Helpilepsy	✓	-	✓	-	-	-
Epsy	✓	✓	✓	✓	-	-
Proposed work*	✓	✓	✓	✓	✓	✓

Table 6.1: Mainstream Application with functionalities. *:Real-time recording function is based on simulation of EEG.

The mainstream epilepsy health apps currently on the market do have some limitations. Firstly, the epilepsy knowledge sharing function is not adequately represented in most software. This may prevent patients and their families from obtaining necessary information about epilepsy, such as symptom recognition, treatment options, and responses in case of emergency. The lack of knowledge may result in patients not being able to effectively participate in their own treatment process, thus affecting disease management and quality of life.

Another significant limitation is the lack of real-time neuroimaging visualization capabilities. Currently, neuroimaging results can usually only be viewed at a healthcare professional's endpoint, and patients do not have direct access to this

information. This situation stems in part from the complexity of neuroimaging results and the background of medical knowledge required, making it difficult for patients to interpret them on their own. As a result, this function is not currently a major need for the patient community. However, as AI technology continues to evolve and become more widespread, the likelihood that patients can interpret medical results on their own is increasing. This function has the potential to be useful in the future.

Based on the above discussion, the proposed app in this work will endeavor to integrate all features including Neuro-Recording to comprehensively meet the epilepsy management needs of patients. Our app will not only aim to provide existing useful functions but will also explore the innovations that AI technology may bring in the future. In terms of software design, we will focus on innovation and novelty, avoiding traditional design elements. We believe that a modern user interface can enhance the user experience and enable users to manage their health more easily.

It should be noted that due to time constraints and technical limitations, the medical results presented in the software will be simulation-based examples. This means that while we endeavor to provide an experience that is close to real medical data, users should be aware that this data is for demonstration purposes only and does not represent real medical advice or diagnosis.

6.3.3 Technical Details

In the context of mobile application design, the proposed application is defined to run on the Android operating system. However, Android is not the only mainstream operating system in the current diverse technology ecosystem. Cross-platform compatibility for future development is an important consideration. This not only expands the user base, but also reduces maintenance costs and improves the software's competitiveness in the market.

Flutter is an application design framework launched by Google and is known for its excellent cross-platform compatibility. It is written in the Dart language and supports hot reloading features, which can significantly improve development efficiency. Flutter enables developers to easily build high-performance, consistently styled cross-platform applications through its rich component library and highly customizable features. In this work, we chose Flutter as the application running framework to achieve the goal of efficient and compatible development. Therefore, in this work, we choose Flutter as the program running framework to achieve the goal of efficient and compatible development.

To develop and test the mobile application, we used Android Studio, an integrated development environment (IDE). Android Studio, as developed by JetBrains, is currently the most mainstream Android application development tool. It provides powerful code editing, debugging and performance analysis functions, which can effectively improve development efficiency and application quality. Therefore, Android Studio was the ideal choice when we chose it as our IDE.

During the development of the NeuroSafe mobile application, we faced the challenge of real-time data acquisition and refreshing. Flutter supports the introduction and use of third-party libraries, like Java's Gradle and Python's Pip, which greatly simplifies the development process of mobile applications.

In the proposed mobile application, we mainly used the following two libraries: Redis (version 4.0.0) and Flchart (version 0.67.0). The Redis library is used to connect to a remote Redis database and supports a variety of operations on the database(*Redis | Dart Package*, n.d.). It is used by mobile applications to fetch blocks of data stored temporarily on the database, while the Flchart library is used to display aesthetically pleasing charts and graphs, with support for animation and custom formatting(*Fl_chart | Flutter Package*, n.d.). It is used by mobile applications to display real-time brain signals.

Specifically, the mobile application uses the Redis plugin to fetch data blocks from the database at regular intervals of 500 milliseconds, and the data blocks are processed into a time series. the UI interface is refreshed at 800 milliseconds and rendered using Flchart. The UI refresh rate will be slightly slower than the data fetching rate due to the slow rendering speed of the UI interface.

The full list of packages and libraries used in this work can be found in Appendix C, while information on the configuration of the development and testing environments can be found in Appendix D.

6.3.4 Functions and User Interface Design

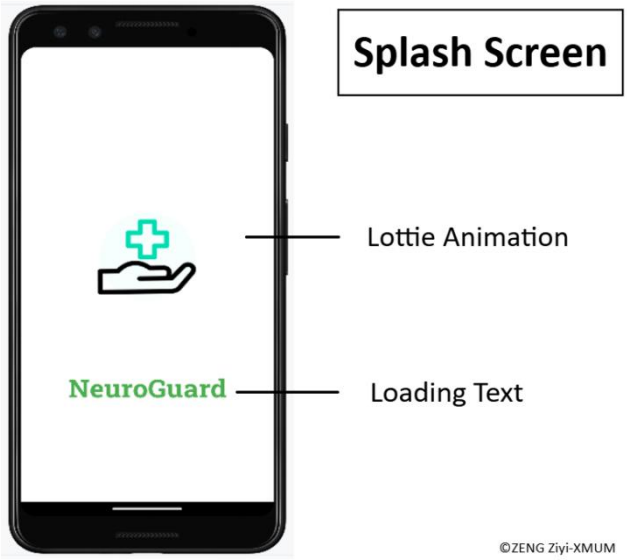

Figure 6.4: UI Design on Splash Screen

Figure 6.4 shows the opening animation of the applications, which was realized by the Lottie package. During the initialization process, this opening animation not only prevents the user from getting bored, but also significantly improves the overall user experience.

The design of the opening animation is unique in that it contains the elements of a

hand and a medical icon, which ties in with the theme of the software and symbolizes health and care. The animation is smooth and visually appealing, allowing users to feel the professionalism and user-friendliness of the software while waiting for it to initialize. After the animation, a well-written callback function will be automatically launched to seamlessly guide the user to the main interface. With this opening animation, the software leaves a deep impression in the user's mind, laying a good foundation for the next experience.

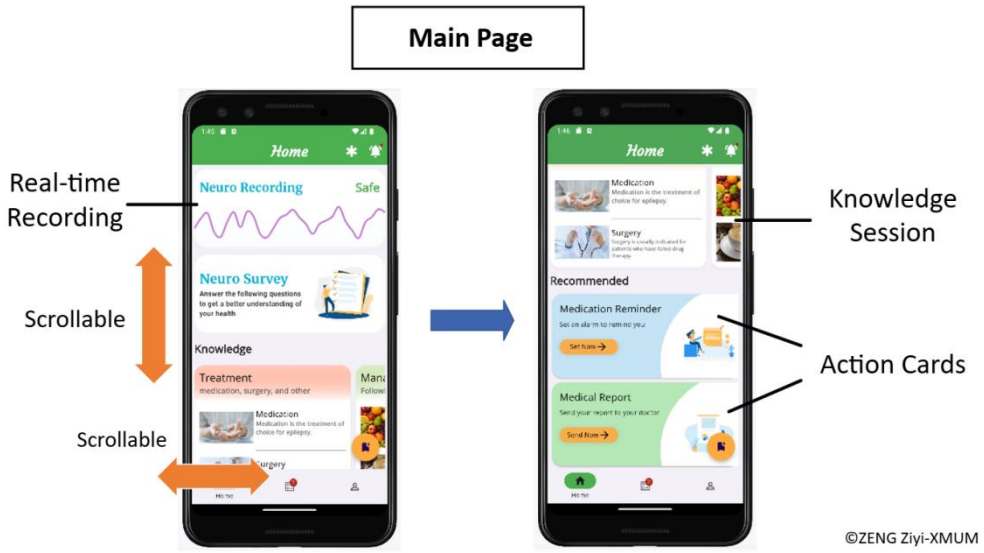

Figure 6.5: UI Design on Main Page

The main page showcases the core functionality of the software, providing a wealth of features for the user to explore. Users can easily access each section by simply swiping up and down the screen. Firstly, at the top of the main page is an eye-catching control that displays Neuro Recording in real time, refreshing the data every 3 seconds. This data comes from sophisticated neuroimaging equipment, providing patients with instant feedback on their neural signals. Immediately following this, the second control is a well-designed questionnaire prompt that will kindly remind the user to complete the questionnaire to assess their health status.

Upon clicking, the user is seamlessly guided to the questionnaire page, which will be described in detail in subsequent sections.

In the middle of the interface is the Knowledge Panel, which displays content by sliding horizontally. This feature is achieved through a well-designed ListView. The board contains three cards that deal with epilepsy prevention, treatment, and daily maintenance. Under each card are two sub-topics that provide more specific and practical health information. This hierarchical knowledge structure ensures efficient reading while maintaining the clarity and ease of use of the interface.

At the bottom of the page is the Recommendations section, which contains several well-designed action cards that provide personalized suggestions for further action. Among them, "Medication Reminder" is a sweet feature to remind users to take medication on time. Clicking on the card will pop up a user-friendly time setting box, allowing the user to easily set the time for taking the medication. Additionally, patients can generate a detailed epilepsy report from the medical data recorded by the software with one click and send it to the appropriate doctor. This feature is available in the "Medical report" card. After clicking on the card, the app automatically generates the report and allows the user to select a doctor. With just one click, the medical report can be sent to the doctor, allowing the patient to get professional medical advice in a timely manner.

To further enhance the scope of our services, we have crafted a new feature, the Epilepsy News page, and integrated it into our mobile app. This page, as a separate functional module, provides users with the latest news and information on epilepsy. Users can easily access the news page by simply touching the bottom menu bar.

Figure 6.6 shows the UI design of the news page. When visiting the news page for the first time, the system will initialize and get the latest news data in real time. To enhance the user experience, we designed a rotating progress bar during the data

loading process to remind the user that the data is being loaded and make the waiting more intuitive. Once data loading is complete, the software will automatically display the latest epilepsy news. This news information is sourced from the reliable News API, ensuring that the information is accurate and up to date. Users can easily update the content on the news page with a simple drop-down gesture to get the latest information.

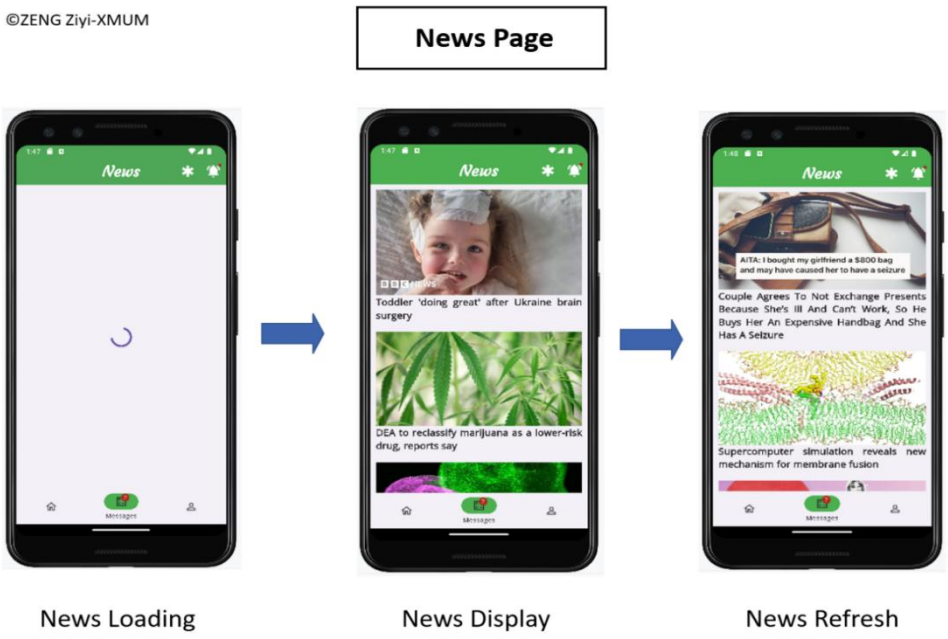

Figure 6.6: UI Design on News Page

Each story on the News page is carefully displayed with headlines and accompanying images, allowing users to quickly capture the gist of the news. Users who are interested in a particular news item can simply click on the corresponding image to get detailed information about the news. Once clicked, the software will intelligently navigate the user to a specific news website where the user can enjoy reading the full article. This feature not only provides users with a wealth of information resources, but also enhances the interactive experience between users and the software.

For patients who have epilepsy, it is crucial to monitor their health in real time. Hence, our carefully designed Epilepsy Assessment feature was created to help patients better manage their health. The feature provides a comprehensive assessment of the patient's current health status and predicts the likelihood of future seizures through a series of well-designed questionnaires.

Patients can easily access the assessment screen from the main screen. Figure 6.7 illustrates the UI design and jump logic of the epilepsy assessment interface. The entire assessment consists of 6 targeted questions designed to provide a comprehensive understanding of the patient's health status. First, the interface displays the patient's most recent assessment record and highlights the score of the most recent assessment. A higher score indicates that the patient is at lower risk for future seizures, a message that provides peace of mind and confidence.

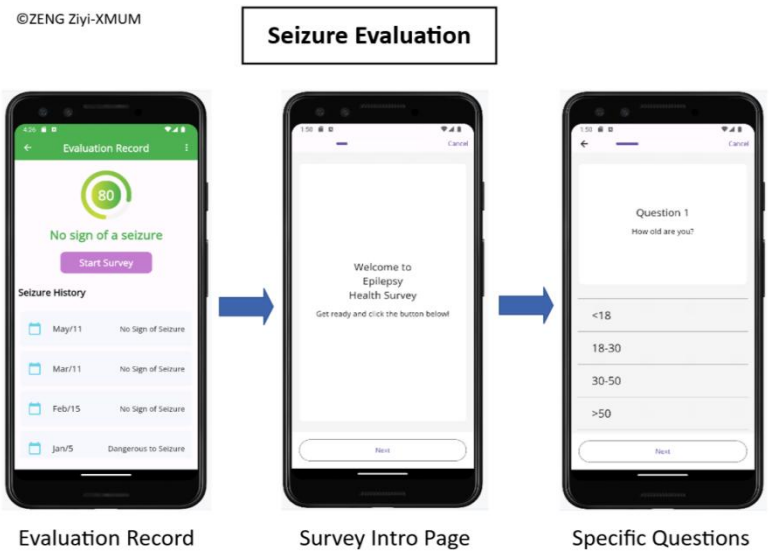

Figure 6.7: UI design on seizure evaluation

To enhance the user experience, the record display supports swipe up and down operations, allowing users to easily navigate through historical assessment results. When the patient is ready for a new assessment, simply click the button to start the

assessment process. A questionnaire page will be presented, and the user will need to follow the guidelines and carefully fill in each question. Once all questions have been answered, the software will automatically close the assessment page and direct the user back to the results page. The results page will display the assessment results in a clear and intuitive way, allowing patients to quickly understand their health status. This function not only provides patients with timely health assessment, but also encourages them to actively participate in health management, thereby reducing the risk of seizures.

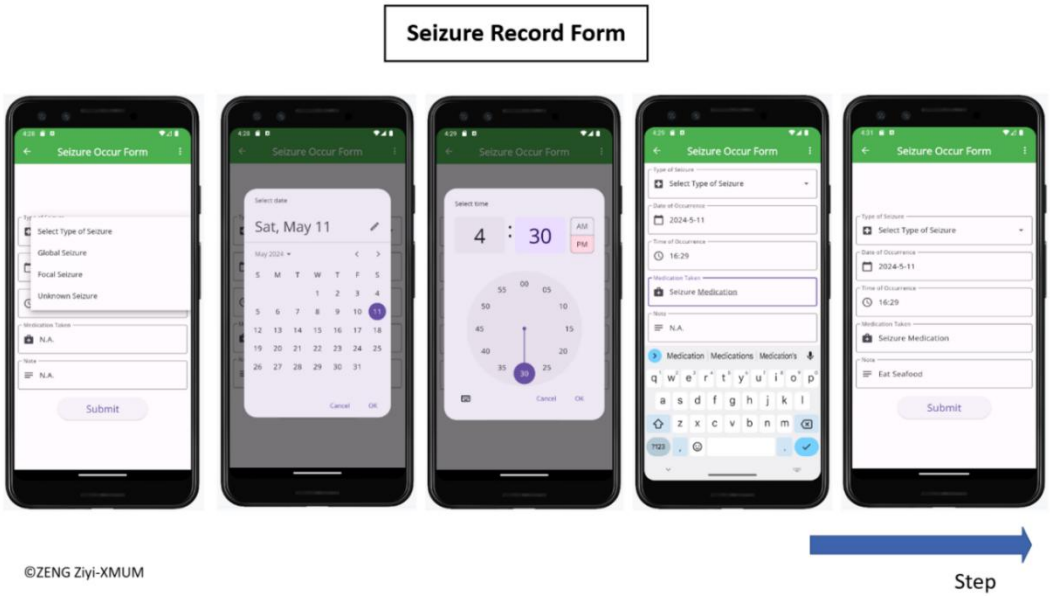

Figure 6.8: UI design on Seizure Record

In daily life, epilepsy patients often need to record the details of each seizure so that doctors can use this information to develop a more effective treatment plan. To simplify this process, our software has introduced a special seizure recording function, which can be easily accessed by patients by simply touching the hover button at the bottom right corner of the main page.

Figure 6.8 illustrates the operational logic of the seizure recording page. The application was designed with a set of concise forms that guided the patient to fill in five key seizure items, three of which were mandatory and two of which were

optional. This information includes seizure type, date, time, medication use, and notes. Each piece of information is designed to help doctors diagnose and treat more accurately. During the filling process, patients can select the type of seizure according to their situation, enter the exact date and time of the seizure, as well as the medication used at the time. If needed, patients can also add any additional information in the notes field, such as activities, diet, or mood changes prior to the seizure.

Once the patient has filled in all the necessary information and clicked submit, the software will automatically save these records. In this way, the patient creates a detailed seizure log, providing a valuable information resource for the physician. On the “Occurrence Record” page, the patient can view and review these saved seizures at any time, a feature that will be described in more detail in a subsequent section. In this way, patients can not only better manage their own health status, but also provide doctors with accurate treatment basis, which can jointly promote the improvement of treatment results.

The design of the settings page is shown in Figure 6.9, which is carefully divided into three main sections: user information, notification settings, and epilepsy records so that users can easily manage and adjust their personal settings. In the user information section, the page displays the basic information of the currently logged-in user in the form of a user card, including personalised details such as user avatar and username. The user simply touches the card to view more details such as contact information, age, gender, etc., which helps the doctor understand the patient's background in a more comprehensive way.

Following immediately below the user's card are the notification settings, a section that allows the user to customize how they receive notifications. Notification settings are divided into two subcategories: alarm notifications and general notifications. Users can choose the appropriate alert method for each type of notification, such as

sound, vibration, or pop-up window, to ensure that they don't miss any important health reminders or emergencies.

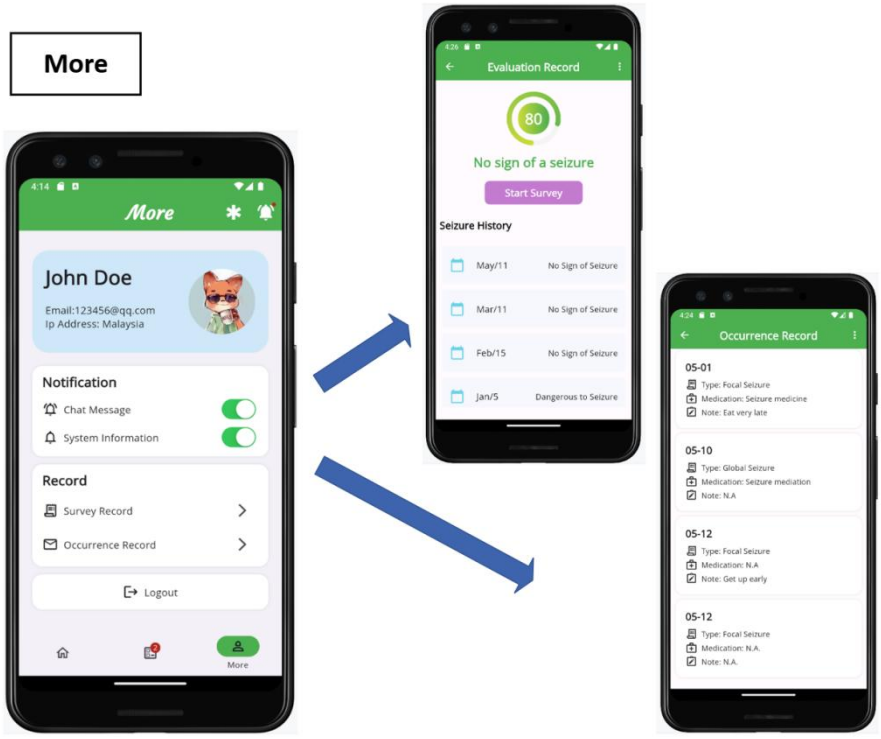

Figure 6.9: UI design on Seizure Record

The middle of the page concentrates on the medical data recording controls. Here, the software integrates the collected medical data, which can be easily viewed and managed by the user. Firstly, there is the 'Survey record' which, when clicked, directs the user to a new page with detailed records of previous evaluations, which can help the user to track changes in health status (see Section 6.3.4).

When the user clicks on "Occurrence record", the software directs the user to a new screen that lists all the episodes manually recorded by the user. This information is essential for the doctor's diagnosis and treatment planning. For further convenience, the software is designed to generate and send medical reports. Patients can generate detailed medical reports with a single click and send them directly to their doctors through the software for professional medical advice and further support.

Chapter 7: Conclusion of Thesis

As the final chapter of the thesis, this chapter will summarize the previous section.

Firstly, the paper opens with a definition and treatment of epilepsy and outlines the importance of automated epilepsy detection algorithms. Epilepsy detection algorithms have a promising application as they can reduce the workload of medical professionals and ensure timely response. Subsequently, this paper provides an overview of existing research efforts in the field of epilepsy, pointing out that epilepsy detection latency is an important metric that has been overlooked in many research endeavors. Therefore, this study presents a series of potential factors that may affect this metric.

To delve deeper into the impact of each potential factor on detection delay, multiple solutions are proposed in this paper. The findings corresponding to each hypothesis are listed in Table 7.1. Firstly, this paper proposes three feature extractor architectures, and experimentally demonstrates that an increase in the size of the feature extractor leads to a slight improvement in model performance but may be accompanied by a decrease in model stability. Subsequently, this paper delves into the hybrid feature extractor, and the experimental results show that combining convolutional neural network and Transformer can effectively improve the detection delay.

In addition, this paper demonstrates for the first time the usefulness of the sliding window technique in improving the detection delay. Specifically, after shortening the sliding window to 2 seconds, the detection latency improves to 1.82 seconds, which is currently the best latency value in the field of epilepsy detection. However, due to the lack of controlled experiments and ablation experiments, this paper is still unable to determine the validity of this metric, and thus further validation is still needed for subsequent studies.

As a complement to this study, this paper presents a closed-loop real-time neuroimaging monitoring system (C-RNMS) based on a mobile application. The system consists of three components: a neuroimaging acquisition system, an artificial intelligence cloud computing platform, and a mobile health application. The proposed system is expected to lower the threshold of neuroimaging technology and help epilepsy patients better monitor and understand their condition.

Potential Factor	Methodology	Improvement
Model Size	Proposed and evaluate FE with different scales	Slight
Model Structure	1) Proposed and evaluate FE base on different structure 2) Proposed and evaluate hybrid FE	Significant
EEG Normalization	Evaluate the result with and without normalization	Negligible
Length of Slicing Windows	Evaluate hybrid model on 2 seconds slicing windows	Significant

Table 7.1: Potential Factor, Proposed Methodology, and Improvement in Detection Latency

In order to achieve a floor-ready, high-performing epilepsy detection algorithm, such an algorithm should be effective for all patients, without the need to acquire patient-specific EEG segments. Therefore, one of the important directions for future research on epilepsy algorithms is to build a cross-patient detection algorithm that does not rely on patient-specific EEG segments. In addition, assessing the goodness of an algorithm should be multivariate and not rely on a single metric. Therefore, another research direction is to comprehensively improve the overall performance of the algorithm.

Finally, may all epilepsy patients get well soon and stay away from the disease.

Appendix

A. Supplementary Experiments

A1. Spectrogram Normalization

Patient_id	w/o Spectrogram Normalization			Spectrogram Normalization		
	acc	f1	auc	acc	f1	auc
1	**0.86(0.18)**	0.76(0.34)	0.89(0.18)	0.85(0.22)	0.72(0.43)	0.88(0.20)
2	**0.63(0.14)**	0.32(0.34)	0.67(0.17)	0.62(0.12)	0.34(0.28)	0.78(0.09)
3	0.87(0.16)	0.79(0.31)	0.91(0.16)	**0.93(0.08)**	0.92(0.10)	0.97(0.04)
5	0.82(0.17)	0.71(0.31)	0.87(0.15)	**0.82(0.11)**	0.75(0.20)	0.89(0.10)
9	**0.74(0.18)**	0.58(0.35)	0.82(0.17)	0.67(0.20)	0.39(0.41)	0.70(0.20)
10	**0.73(0.13)**	0.61(0.23)	0.78(0.14)	0.70(0.17)	0.50(0.35)	0.76(0.18)
14	0.52(0.04)	0.18(0.12)	0.56(0.08)	**0.54(0.08)**	0.27(0.26)	0.56(0.11)
18	0.80(0.17)	0.68(0.33)	0.88(0.14)	**0.84(0.19)**	0.76(0.32)	0.88(0.16)
19	**0.77(0.20)**	0.59(0.42)	0.82(0.23)	0.67(0.13)	0.44(0.30)	0.79(0.16)
20	**0.90(0.20)**	0.80(0.40)	0.90(0.20)	0.89(0.20)	0.79(0.40)	0.90(0.20)
21	0.61(0.10)	0.39(0.23)	0.68(0.13)	**0.62(0.11)**	0.42(0.24)	0.70(0.13)
22	0.55(0.03)	0.20(0.11)	0.61(0.06)	**0.60(0.09)**	0.34(0.22)	0.66(0.11)
23	**0.90(0.09)**	0.87(0.12)	0.94(0.04)	0.88(0.04)	0.86(0.05)	0.94(0.04)

Table A1: Performance Comparison with and without Spectrogram Normalization

Table 10 shows the Performance Comparison with and without Spectrogram Normalization on seizure prediction task. As shown in the table, the difference in performance between the normalized and untreated Spectrogram on the validation set is not significant. Specifically, the untreated Spectrogram achieved better results on the data from seven patients, while it was inferior to the normalized one on another six patients.

This result suggests that the normalization of the Spectrogram may have a limited effect on model performance enhancement, or that its effect may vary on different datasets. With this in mind, we decided not to normalize the Spectrogram in subsequent experiments.

A2. Comparison on Transformer Performance with Different Scheduler

Patient	w Linear Scheduler		w Warm-up Cosine Scheduler	
	Delay	Sensitivity	Delay	Sensitivity
1	**2.60**	7/7	2.61	7/7
2	**7.57**	3/3	8.05	3/3
3	3.00	7/7	**2.92**	7/7
5	5.35	3/4	**4.74**	3/4

Table A2: Performance Comparison using Different Learning Rate Scheduler

Table 11 demonstrates the performance comparison of the transformer model on epilepsy data from four patients under two different learning rate tuners. The warm-up strategy is a commonly used learning rate tuning method designed to help the model converge faster in the early stages of training and to avoid skipping the optimal solution due to too large a learning rate in the later stages of training. However, in this experiment, the transformer model with the warm-up strategy did not achieve leading performance on all samples, which is inconsistent with the conclusions drawn by some existing work (L. Liu et al., 2019). This discrepancy may be due to the following two reasons:

- Sample size: a single seizure from a patient is only about half a minute or so long, and the number of samples generated may not be enough for the model to learn enough features. This does not fully demonstrate where the advantages of the warm-up strategy lie.

- Dataset characteristics: this experiment uses the CHB-MIT, and the warm-up strategy may not perform well on this dataset. However, it does not exclude the possibility that this strategy can help the model to find a good solution on other datasets.

Even though the warm-up strategy did not show a clear advantage in this experiment, this learning rate adjuster was still employed in the remaining experiments out of caution. This is because the warm-up strategy has been shown to be effective in many cases, and it provides a relatively safe starting point for model training, helping to avoid model instability due to excessive learning rates in the early stages of training.

A3. Comparison on Hybrid Feature Extractor

Model	Double Conv-Large		Conv-Large & Transf-Large		Conv-Large & Transf-Small		Rec-Small & Transf-Small		Rec-Large & Transf-Small	
Patient ID	*Latency*	*Sen*	*Latency*	*Sen*	*Latency*	*Sen*	*Latency*	*Sen*	*Latency*	*Sen*
1	3.13(2.87)	7/7	2.59(2.07)	7/7	3.00(2.19)	7/7	2.61(1.90)	7/7	**2.43(1.81)**	7/7
2	6.01(3.24)	3/3	**6.43(4.06)**	3/3	6.01(3.96)	3/3	7.42(5.81)	3/3	7.83(6.64)	3/3
3	2.73(1.85)	7/7	**2.88(1.73)**	7/7	3.25(2.10)	7/7	3.02(2.00)	7/7	3.05(2.19)	7/7
4	**4.50(2.26)**	3/4	5.33(4.04)	3/4	5.14(4.03)	3/4	4.58(3.48)	3/4	4.61(3.36)	3/4
5	4.19(3.31)	5/5	4.18(2.43)	5/5	4.60(1.94)	5/5	3.77(3.07)	5/5	**3.63(2.90)**	5/5
6	2.21(0.31)	10/10	**2.42(0.21)**	10/10	2.49(0.23)	10/10	2.54(0.11)	10/10	2.47(0.10)	10/10
7	3.51(0.66)	3/3	**3.65(0.32)**	3/3	5.76(3.54)	3/3	5.29(3.07)	3/3	5.18(3.26)	3/3
8	**2.15(1.70)**	5/5	3.43(3.27)	5/5	4.36(3.66)	5/5	4.53(2.98)	5/5	3.87(2.90)	5/5
9	3.03(0.80)	4/4	5.20(4.70)	4/4	5.39(5.14)	4/4	**4.40(4.44)**	4/4	4.45(4.31)	4/4
10	2.76(1.79)	7/7	**1.96(1.68)**	7/7	2.65(1.70)	7/7	2.92(1.96)	7/7	2.15(1.87)	7/7
11	1.68(1.66)	2/3	**0.02(0.0)**	2/3	**0.02(0.0)**	2/3	0.90(0.88)	2/3	0.88(0.85)	2/3
14	5.58(3.46)	8/8	4.75(1.07)	8/8	4.78(1.00)	8/8	**3.60(1.48)**	8/8	3.60(1.62)	8/8
17	**4.47(2.73)**	3/3	5.17(0.62)	3/3	5.29(0.88)	3/3	5.85(1.34)	3/3	6.56(0.83)	3/3
18	4.74(6.82)	5/6	4.09(3.39)	5/6	**3.93(2.48)**	5/6	5.65(6.75)	5/6	9.37(8.83)	5/6

19	4.47(2.64)	3/3	**2.73(0.70)**	3/3	3.99(0.24)	3/3	2.79(0.61)	3/3	2.94(0.98)	3/3
20	2.90(2.80)	8/8	4.07(2.23)	8/8	4.06(2.42)	8/8	3.63(2.20)	8/8	**3.59(2.20)**	8/8
21	3.93(3.68)	4/4	2.57(1.88)	4/4	**1.19(1.16)**	4/4	2.29(1.44)	4/4	1.96(1.83)	4/4
22	8.08(4.36)	3/3	6.40(3.38)	3/3	9.48(4.74)	3/3	**5.74(3.53)**	3/3	8.10(4.07)	3/3
23	2.66(2.35)	7/7	2.97(2.37)	7/7	2.43(1.89)	7/7	**1.78(1.41)**	7/7	2.08(1.5)	7/7
Total	3.82(2.59)	97/100	**3.72(2.11)**	97/100	4.09(2.27)	97/100	3.85(2.55)	97/100	4.14(2.73)	97/100

Table A3: Performance Comparison on All Hybrid Extractor. Format: Mean(Std)

B. Model Training Time Estimation

The computational idea of the full model is to use Transformer FE (small) as the baseline, and the actual training time is obtained by corresponding scaling and computation according to the number of parameters corresponding to the actual model.

Transformer -base FE (small) The computational time in each seizure training can be divided into multiple parts as shown in Table A4:

Component	Count	Estimate Epoch Time	Estimate Total Time
Data Preparation	1	40	40 seconds
Training Epoch	30	1.5	45 seconds
Validation Epoch	3	1.5	4.5 seconds
Evaluation Epoch	1	8	8 seconds
Latency Test	1	20	20 seconds
Total			117.5 seconds

Table A4: Training Time Evaluation of Each Phase

There are 100 seizures in the entire dataset, so the total training time is 117.5*100 seizures = 11,750 seconds, which is 195.8 minutes. Scaling this up gives the time required for the full model training.

C. Flutter Package Used in Application Design

Package Name	Version	Description
google_fonts	6.2.1	A package to support google font displaying
lottie	3.1.0	A popular animation play package
form_validator	2.1.1	Simplest form validation for flutter form widgets.
fluttertoast	8.2.5	Toast Library for Flutter
url_launcher	6.2.6	Lauch a call, url or application
fl_chart	0.67.0	highly customizable Flutter chart library
webview_flutter	4.7.0	A Flutter plugin that provides a WebView widget.
survey_kit	1.0.0-dev.6	A library Create beautiful surveys with Flutter
redis	4.0.0	Redis protocol parser and client for Dart

Table 10: Performance Comparison with and without Spectrogram Normalization

D. Environment for Application Developing and Debug

The environment for mobile application developing is listed as below:

- Operating System: Wondows 11 24H2
- IDE: Jetbrain Android Studio 2023.3 (Jellyfish)

- Android API Level: 34
- Android SDK: Android 14 (UpDownCake)
- Android Emulator: 34.2.13
- Rendering Device (Display Card): Geforce RTX 4060

E. Final Year Project Breakdown

a) Proposal Version

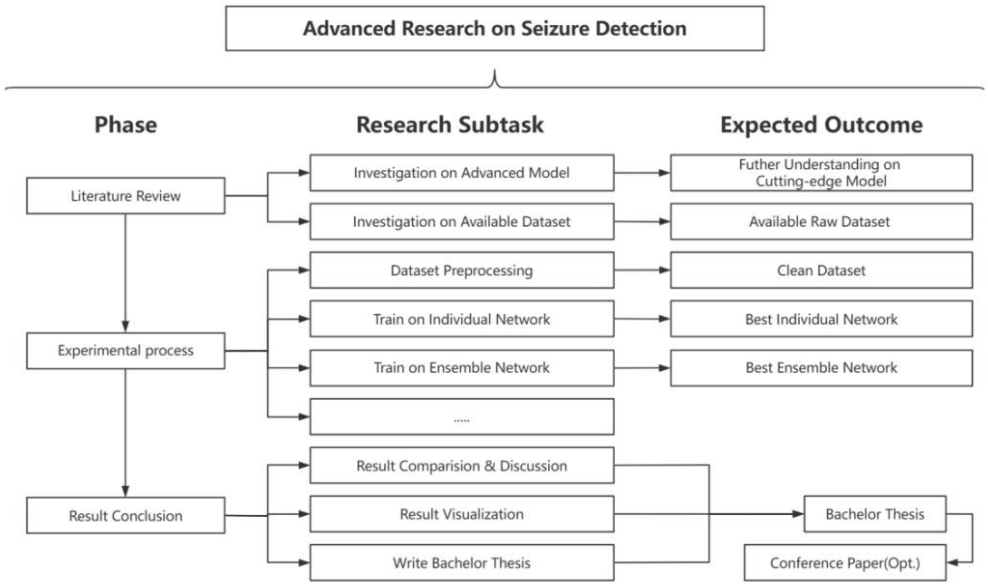

Figure A1: Final Year Project Breakdown (Proposal Version)

b) Final Version

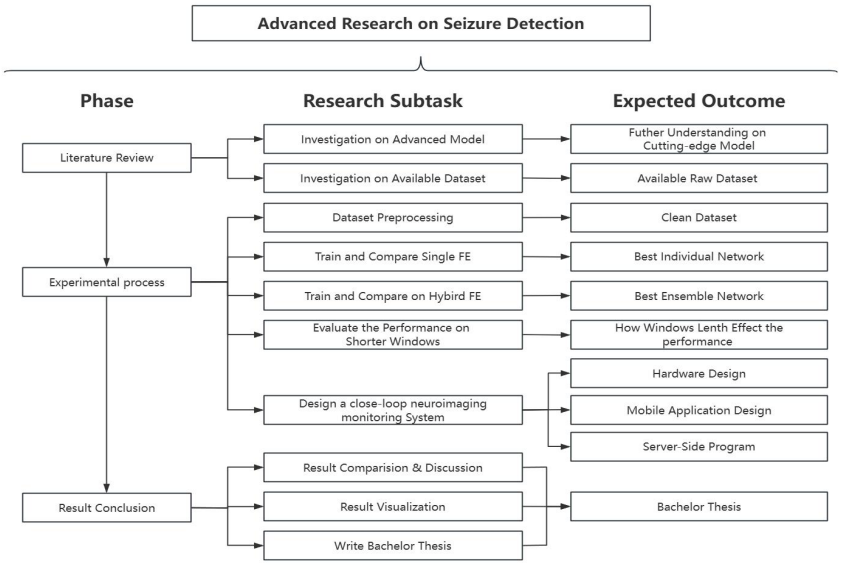

Figure A2: Final Year Project Breakdown (Thesis Version)

F. Completion of Proposal Milestone

Stage	Task Name	Completion	Remark
1	Overall Literature Review	✔	
	Datasets Pre-processing	✔	
2	Train each of FE	✔	
	Evaluate each FE	✔	
	Overall Evaluation	✔	
	Evaluation on Shorter Slicing Windows	✔	Extra-work
	Real Use Case Evaluation	✔	Extra-work
	RNMS Hardware Design	✔	Extra-work
	RNMS Mobile Application	✔	Extra-work
3	Conclude experiment result	✔	
	Formal Thesis	✔	

Table A5: Completion of Proposal Milestone

Reference

Alzamanan, M. Z., Lim, K.-S., Akmar Ismail, M., & Abdul Ghani, N. (2021). Self-Management Apps for People With Epilepsy: Systematic Analysis. *JMIR mHealth and uHealth*, *9*(5), e22489. https://doi.org/10.2196/22489

Asif, U., Roy, S., Tang, J., & Harrer, S. (2020). *SeizureNet: Multi-Spectral Deep Feature Learning for Seizure Type Classification* (arXiv:1903.03232). arXiv. https://doi.org/10.48550/arXiv.1903.03232

Balabanov, A. K. and A. (2008). Pre-surgical psychiatric evaluations: Risk factors for post-surgical deficits. In *Textbook of Epilepsy Surgery*. CRC Press.

Beniczky, S., & Schomer, D. L. (2020a). Electroencephalography: Basic biophysical and technological aspects important for clinical applications. *Epileptic Disorders: International Epilepsy Journal with Videotape*, *22*(6), 697–715. https://doi.org/10.1684/epd.2020.1217

Beniczky, S., & Schomer, D. L. (2020b). Electroencephalography: Basic biophysical and technological aspects important for clinical applications. *Epileptic Disorders: International Epilepsy Journal with Videotape*, *22*(6), 697–715. https://doi.org/10.1684/epd.2020.1217

Bhattacharya, A., Baweja, T., & Karri, S. P. K. (2022). Epileptic Seizure Prediction Using Deep Transformer Model. *International Journal of Neural Systems*, *32*(2), 2150058. https://doi.org/10.1142/S0129065721500581

Birjandtalab, J., Heydarzadeh, M., & Nourani, M. (2017). Automated EEG-Based Epileptic Seizure Detection Using Deep Neural Networks. *2017 IEEE International Conference on Healthcare Informatics (ICHI)*, 552–555. https://doi.org/10.1109/ICHI.2017.55

Brigham, E. O., & Morrow, R. E. (1967). The fast Fourier transform. *IEEE Spectrum*, *4*(12), 63–70. https://doi.org/10.1109/MSPEC.1967.5217220

Bullmore, E., & Sporns, O. (2009). Complex brain networks: Graph theoretical

analysis of structural and functional systems. *Nature Reviews Neuroscience*, *10*(3), 186–198. https://doi.org/10.1038/nrn2575

Burrello, A., Benatti, S., Schindler, K., Benini, L., & Rahimi, A. (2021). An Ensemble of Hyperdimensional Classifiers: Hardware-Friendly Short-Latency Seizure Detection With Automatic iEEG Electrode Selection. *IEEE Journal of Biomedical and Health Informatics*, *25*(4), 935–946. https://doi.org/10.1109/JBHI.2020.3022211

Burton, A. (2018). How do we fix the shortage of neurologists? *The Lancet. Neurology*, *17*(6), 502–503. https://doi.org/10.1016/S1474-4422(18)30143-1

Chami, I., Abu-El-Haija, S., Perozzi, B., Ré, C., & Murphy, K. (2022). *Machine Learning on Graphs: A Model and Comprehensive Taxonomy* (arXiv:2005.03675). arXiv. https://doi.org/10.48550/arXiv.2005.03675

Chen, Y.-H., Yang, J., Hemmings Wu, Beier, K. T., & Sawan, M. (2023). Challenges and future trends in wearable closed-loop neuromodulation to efficiently treat methamphetamine addiction. *Frontiers in Psychiatry*, *14*, 1085036. https://doi.org/10.3389/fpsyt.2023.1085036

Cimr, D., Fujita, H., Tomaskova, H., Cimler, R., & Selamat, A. (2023). Automatic seizure detection by convolutional neural networks with computational complexity analysis. *Computer Methods and Programs in Biomedicine*, *229*, 107277. https://doi.org/10.1016/j.cmpb.2022.107277

Covert, I., Krishnan, B., Najm, I., Zhan, J., Shore, M., Hixson, J., & Po, M. J. (2019). *Temporal Graph Convolutional Networks for Automatic Seizure Detection* (arXiv:1905.01375). arXiv. http://arxiv.org/abs/1905.01375

Debnath, L., & Antoine, J.-P. (2003). Wavelet Transforms and Their Applications. *Physics Today - PHYS TODAY*, *56*, 68–68. https://doi.org/10.1063/1.1580056

Dosovitskiy, A., Beyer, L., Kolesnikov, A., Weissenborn, D., Zhai, X., Unterthiner, T., Dehghani, M., Minderer, M., Heigold, G., Gelly, S., Uszkoreit, J., & Houlsby,

N. (2020). An Image is Worth 16x16 Words: Transformers for Image Recognition at Scale. *ArXiv*. https://www.semanticscholar.org/paper/An-Image-is-Worth-16x16-Words%3A-Transformers-for-at-Dosovitskiy-Beyer/268d347e8a55b5eb82fb5e7d2f800e33c75ab18a

Dosovitskiy, A., Beyer, L., Kolesnikov, A., Weissenborn, D., Zhai, X., Unterthiner, T., Dehghani, M., Minderer, M., Heigold, G., Gelly, S., Uszkoreit, J., & Houlsby, N. (2021). *An Image is Worth 16x16 Words: Transformers for Image Recognition at Scale* (arXiv:2010.11929). arXiv. https://doi.org/10.48550/arXiv.2010.11929

Fisher, R. S., Cross, J. H., French, J. A., Higurashi, N., Hirsch, E., Jansen, F. E., Lagae, L., Moshé, S. L., Peltola, J., Roulet Perez, E., Scheffer, I. E., & Zuberi, S. M. (2017). Operational classification of seizure types by the International League Against Epilepsy: Position Paper of the ILAE Commission for Classification and Terminology. *Epilepsia*, *58*(4), 522–530. https://doi.org/10.1111/epi.13670

Fl_chart | Flutter package. (n.d.). Retrieved 11 June 2024, from https://pub.dev/packages/fl_chart

Goldenberg, M. M. (2010). Overview of drugs used for epilepsy and seizures: Etiology, diagnosis, and treatment. *P & T: A Peer-Reviewed Journal for Formulary Management*, *35*(7), 392–415.

Gramfort, A., Luessi, M., Larson, E., Engemann, D., Strohmeier, D., Brodbeck, C., Goj, R., Jas, M., Brooks, T., Parkkonen, L., & Hämäläinen, M. (2013). MEG and EEG data analysis with MNE-Python. *Frontiers in Neuroscience*, *7*. https://doi.org/10.3389/fnins.2013.00267

Hassan, A. R., Subasi, A., & Zhang, Y. (2020). Epilepsy seizure detection using complete ensemble empirical mode decomposition with adaptive noise.

Knowledge-Based Systems, *191*, 105333. https://doi.org/10.1016/j.knosys.2019.105333

Hossain, M. S., Amin, S. U., Alsulaiman, M., & Muhammad, G. (2019). Applying Deep Learning for Epilepsy Seizure Detection and Brain Mapping Visualization. *ACM Transactions on Multimedia Computing, Communications, and Applications*, *15*(1s), 10:1-10:17. https://doi.org/10.1145/3241056

Hu, S., Liu, J., Yang, R., Wang, Y., Wang, A., Li, K., Liu, W., & Yang, C. (2023). Exploring the Applicability of Transfer Learning and Feature Engineering in Epilepsy Prediction Using Hybrid Transformer Model. *IEEE Transactions on Neural Systems and Rehabilitation Engineering*, *31*, 1321–1332. https://doi.org/10.1109/TNSRE.2023.3244045

Hyvärinen, A., & Oja, E. (2000). Independent component analysis: Algorithms and applications. *Neural Networks*, *13*(4), 411–430. https://doi.org/10.1016/S0893-6080(00)00026-5

Jana, G. C., Agrawal, A., Pattnaik, P. K., & Sain, M. (2022). DWT-EMD Feature Level Fusion Based Approach over Multi and Single Channel EEG Signals for Seizure Detection. *Diagnostics*, *12*(2), Article 2. https://doi.org/10.3390/diagnostics12020324

Kamousi, B., Grant, A., Bachelder, B., Yi, J., Hajinoroozi, M., & Woo, R. (2019). Comparing the quality of signals recorded with a rapid response EEG and conventional clinical EEG systems. *Clinical Neurophysiology Practice*, *4*, 69–75. https://doi.org/10.1016/j.cnp.2019.02.002

Kehtarnavaz, N. (2008). CHAPTER 7—Frequency Domain Processing. In N. Kehtarnavaz (Ed.), *Digital Signal Processing System Design (Second Edition)* (pp. 175–196). Academic Press. https://doi.org/10.1016/B978-0-12-374490-6.00007-6

Khuda, I., & Aljaafari, D. (2018). Epilepsy in pregnancy: A comprehensive literature review and suggestions for saudi practitioners. *Neurosciences Journal*, *23*(3), 185–193. https://doi.org/10.17712/nsj.2018.3.20180129

Li, C., Zhou, W., Liu, G., Zhang, Y., Geng, M., Liu, Z., Wang, S., & Shang, W. (2021). Seizure Onset Detection Using Empirical Mode Decomposition and Common Spatial Pattern. *IEEE Transactions on Neural Systems and Rehabilitation Engineering*, *29*, 458–467. https://doi.org/10.1109/TNSRE.2021.3055276

Li, D.-X., Zhou, X.-Y., Lin, Q.-Q., Wu, Y., Hu, C., Shen, Z.-H., & Wang, Y.-G. (2023). Increased EEG gamma power under exposure to drug-related cues: A translational index for cue-elicited craving in METH-dependent individuals. *BMC Psychiatry*, *23*(1), 367. https://doi.org/10.1186/s12888-023-04892-9

Li, Z., Hwang, K., Li, K., Wu, J., & Ji, T. (2022). Graph-generative neural network for EEG-based epileptic seizure detection via discovery of dynamic brain functional connectivity. *Scientific Reports*, *12*(1), 18998. https://doi.org/10.1038/s41598-022-23656-1

Lin, T.-Y., Goyal, P., Girshick, R., He, K., & Dollár, P. (2018). *Focal Loss for Dense Object Detection* (arXiv:1708.02002). arXiv. https://doi.org/10.48550/arXiv.1708.02002

Liu, L., Jiang, H., He, P., Chen, W., Liu, X., Gao, J., & Han, J. (2019). *On the Variance of the Adaptive Learning Rate and Beyond*.

Liu, M., Ren, S., Ma, S., Jiao, J., Chen, Y., Wang, Z., & Song, W. (2021). *Gated Transformer Networks for Multivariate Time Series Classification* (arXiv:2103.14438). arXiv. https://doi.org/10.48550/arXiv.2103.14438

Liu, T., Truong, N. D., Nikpour, A., Zhou, L., & Kavehei, O. (2020). *Epileptic Seizure Classification with Symmetric and Hybrid Bilinear Models* (arXiv:2001.06282). arXiv. http://arxiv.org/abs/2001.06282

Loshchilov, I., & Hutter, F. (2019). *Decoupled Weight Decay Regularization* (arXiv:1711.05101). arXiv. https://doi.org/10.48550/arXiv.1711.05101

Massey, S. L., Jensen, F. E., & Abend, N. S. (2018). Electroencephalographic monitoring for seizure identification and prognosis in term neonates. *Seminars in Fetal and Neonatal Medicine*, *23*(3), 168–174. https://doi.org/10.1016/j.siny.2018.01.001

Myers, M. H., Padmanabha, A., Hossain, G., de Jongh Curry, A. L., & Blaha, C. D. (2016). Seizure Prediction and Detection via Phase and Amplitude Lock Values. *Frontiers in Human Neuroscience*, *10*, 80. https://doi.org/10.3389/fnhum.2016.00080

Noachtar, S. (2018). EEG-Anfallsmuster und Anfallssemiologie. *Klinische Neurophysiologie*, *49*(01), 21–29. https://doi.org/10.1055/s-0043-125297

O'Shea, A., Lightbody, G., Boylan, G., & Temko, A. (2020). Neonatal seizure detection from raw multi-channel EEG using a fully convolutional architecture. *Neural Networks*, *123*, 12–25. https://doi.org/10.1016/j.neunet.2019.11.023

Panayiotopoulos, C. P. (2005a). Optimal Use of the EEG in the Diagnosis and Management of Epilepsies. In *The Epilepsies: Seizures, Syndromes and Management*. Bladon Medical Publishing. https://www.ncbi.nlm.nih.gov/books/NBK2601/

Panayiotopoulos, C. P. (2005b). *The Epilepsies: Seizures, Syndromes and Management*. Bladon Medical Publishing. http://www.ncbi.nlm.nih.gov/books/NBK2606/

Pelin, H., Ising, M., Stein, F., Meinert, S., Meller, T., Brosch, K., Winter, N. R., Krug, A., Leenings, R., Lemke, H., Nenadić, I., Heilmann-Heimbach, S., Forstner, A. J., Nöthen, M. M., Opel, N., Repple, J., Pfarr, J., Ringwald, K., Schmitt, S., … Andlauer, T. F. M. (2021). Identification of transdiagnostic psychiatric

disorder subtypes using unsupervised learning. *Neuropsychopharmacology*, *46*(11), Article 11. https://doi.org/10.1038/s41386-021-01051-0

Rasheed, K., Qayyum, A., Qadir, J., Sivathamboo, S., Kwan, P., Kuhlmann, L., O'Brien, T., & Razi, A. (2021). Machine Learning for Predicting Epileptic Seizures Using EEG Signals: A Review. *IEEE Reviews in Biomedical Engineering*, *14*, 139–155. https://doi.org/10.1109/RBME.2020.3008792

Redis | Dart package. (n.d.). Dart Packages. Retrieved 11 June 2024, from https://pub.dev/packages/redis

Schomer, D. L., & Silva, F. L. da. (2012). *Niedermeyer's Electroencephalography: Basic Principles, Clinical Applications, and Related Fields*. Lippincott Williams & Wilkins.

Shah, V., von Weltin, E., Lopez, S., McHugh, J. R., Veloso, L., Golmohammadi, M., Obeid, I., & Picone, J. (2018). *The Temple University Hospital Seizure Detection Corpus* (arXiv:1801.08085). arXiv. https://doi.org/10.48550/arXiv.1801.08085

Sharma, S., Nunes, M., & Alkhachroum, A. (2022). Adult Critical Care Electroencephalography Monitoring for Seizures: A Narrative Review. *Frontiers in Neurology*, *13*. https://doi.org/10.3389/fneur.2022.951286

Shellhaas, R. A. (2015). Continuous long-term electroencephalography: The gold standard for neonatal seizure diagnosis. *SEMINARS IN FETAL & NEONATAL MEDICINE*, *20*(3), 149–153. https://doi.org/10.1016/j.siny.2015.01.005

Shen, M., Wen, P., Song, B., & Li, Y. (2022). An EEG based real-time epilepsy seizure detection approach using discrete wavelet transform and machine learning methods. *Biomedical Signal Processing and Control*, *77*, 103820. https://doi.org/10.1016/j.bspc.2022.103820

Shen, M., Wen, P., Song, B., & Li, Y. (2023). Real-time epilepsy seizure detection based on EEG using tunable-Q wavelet transform and convolutional neural

network. *Biomedical Signal Processing and Control*, *82*, 104566. https://doi.org/10.1016/j.bspc.2022.104566

Shoeb, A., Edwards, H., Connolly, J., Bourgeois, B., Treves, T., & Guttag, J. (2004). Patient-specific seizure onset detection. *The 26th Annual International Conference of the IEEE Engineering in Medicine and Biology Society*, *1*, 419–422. https://doi.org/10.1109/IEMBS.2004.1403183

Shoeb, A. H. (2009). *Application of machine learning to epileptic seizure onset detection and treatment* [Thesis, Massachusetts Institute of Technology]. https://dspace.mit.edu/handle/1721.1/54669

Shoeb, A. H., & Guttag, J. (2010, June 21). *Application of Machine Learning To Epileptic Seizure Detection*. International Conference on Machine Learning. https://www.semanticscholar.org/paper/Application-of-Machine-Learning-To-Epileptic-Shoeb-Guttag/57e4afe9ca74414fa02f2e0a929b64dc9a03334d

Tang, S., Dunnmon, J., Saab, K. K., Zhang, X., Huang, Q., Dubost, F., Rubin, D., & Lee-Messer, C. (2021, October 6). *Self-Supervised Graph Neural Networks for Improved Electroencephalographic Seizure Analysis*. International Conference on Learning Representations. https://openreview.net/forum?id=k9bx1EfHI_-

Teng, C., & Kravitz, D. J. (2019). Visual working memory directly alters perception. *Nature Human Behaviour*, *3*(8), 827–836. https://doi.org/10.1038/s41562-019-0640-4

Tong, P. F., Zhan, H. X., & Chen, S. X. (2024). Ensembled Seizure Detection Based on Small Training Samples. *IEEE Transactions on Signal Processing*, *72*, 1–14. https://doi.org/10.1109/TSP.2023.3333546

Truong, N. D., Nguyen, A. D., Kuhlmann, L., Bonyadi, M. R., Yang, J., Ippolito, S., & Kavehei, O. (2018). Convolutional neural networks for seizure prediction using intracranial and scalp electroencephalogram. *Neural Networks*, *105*,

104–111. https://doi.org/10.1016/j.neunet.2018.04.018

Urrestarazu, E., Murie, M., & Viteri, C. (2008). Management of first epileptic seizure and status epilepticus in the emergency department. *ANALES DEL SISTEMA SANITARIO DE NAVARRA*, *31*, 61–73.

Vaswani, A., Shazeer, N., Parmar, N., Uszkoreit, J., Jones, L., Gomez, A. N., Kaiser, Ł., & Polosukhin, I. (2017). Attention is all you need. *Proceedings of the 31st International Conference on Neural Information Processing Systems*, 6000–6010.

Vidyaratne, L., Glandon, A., Alam, M., & Iftekharuddin, K. M. (2016). Deep recurrent neural network for seizure detection. *2016 International Joint Conference on Neural Networks (IJCNN)*, 1202–1207. https://doi.org/10.1109/IJCNN.2016.7727334

Vidyaratne, L. S., & Iftekharuddin, K. M. (2017). Real-Time Epileptic Seizure Detection Using EEG. *IEEE Transactions on Neural Systems and Rehabilitation Engineering*, *25*(11), 2146–2156. https://doi.org/10.1109/TNSRE.2017.2697920

Wang, T., Chen, Y.-H., & Sawan, M. (2023). Exploring the Role of Visual Guidance in Motor Imagery-Based Brain-Computer Interface: An EEG Microstate-Specific Functional Connectivity Study. *Bioengineering*, *10*(3), Article 3. https://doi.org/10.3390/bioengineering10030281

Wang, X., Wang, X., Liu, W., Chang, Z., Kärkkäinen, T., & Cong, F. (2021). One dimensional convolutional neural networks for seizure onset detection using long-term scalp and intracranial EEG. *Neurocomputing*, *459*, 212–222. https://doi.org/10.1016/j.neucom.2021.06.048

Wong, S., Simmons, A., Rivera-Villicana, J., Barnett, S., Sivathamboo, S., Perucca, P., Ge, Z., Kwan, P., Kuhlmann, L., Vasa, R., Mouzakis, K., & O'Brien, T. J. (2023). EEG datasets for seizure detection and prediction- A review.

EPILEPSIA OPEN, *8*(2), 252–267. https://doi.org/10.1002/epi4.12704

Xu, Y., Yang, J., Ming, W., Wang, S., & Sawan, M. (2024). Shorter latency of real-time epileptic seizure detection via probabilistic prediction. *Expert Systems with Applications*, *236*, 121359. https://doi.org/10.1016/j.eswa.2023.121359

Xu, Y., Yang, J., & Sawan, M. (2022a). Multichannel Synthetic Preictal EEG Signals to Enhance the Prediction of Epileptic Seizures. *IEEE Transactions on Biomedical Engineering*, *69*(11), 3516–3525. https://doi.org/10.1109/TBME.2022.3171982

Xu, Y., Yang, J., & Sawan, M. (2022b). Trends and Challenges of Processing Measurements from Wearable Devices Intended for Epileptic Seizure Prediction. *Journal of Signal Processing Systems*, *94*(6), 527–542. https://doi.org/10.1007/s11265-021-01659-x

Xu, Y., Yang, J., Zhao, S., Wu, H., & Sawan, M. (2020). An End-to-End Deep Learning Approach for Epileptic Seizure Prediction. *2020 2nd IEEE International Conference on Artificial Intelligence Circuits and Systems (AICAS)*, 266–270. https://doi.org/10.1109/AICAS48895.2020.9073988

Yan, J., Li, J., Xu, H., Yu, Y., & Xu, T. (2022). Seizure Prediction Based on Transformer Using Scalp Electroencephalogram. *Applied Sciences*, *12*(9), 4158. https://doi.org/10.3390/app12094158

Zhang, Z., & Parhi, K. K. (2016). Low-Complexity Seizure Prediction From iEEG/sEEG Using Spectral Power and Ratios of Spectral Power. *IEEE Transactions on Biomedical Circuits and Systems*, *10*(3), 693–706. https://doi.org/10.1109/TBCAS.2015.2477264

Zhao, S., Yang, J., & Sawan, M. (2022). Energy-Efficient Neural Network for Epileptic Seizure Prediction. *IEEE Transactions on Biomedical Engineering*, *69*(1), 401–411. https://doi.org/10.1109/TBME.2021.3095848

Zhao, S., Yang, J., Xu, Y., & Sawan, M. (2020). Binary Single-dimensional Convolutional Neural Network for Seizure Prediction. *2020 IEEE International Symposium on Circuits and Systems (ISCAS)*, 1–5. https://doi.org/10.1109/ISCAS45731.2020.9180430